Chapter 9
Fresh-Water Fluxes via Pacific and Arctic Outflows Across the Canadian Polar Shelf

Humfrey Melling[1], Tom A. Agnew[2], Kelly K. Falkner[3], David A. Greenberg[4], Craig M. Lee[5], Andreas Münchow[6], Brian Petrie[7], Simon J. Prinsenberg[8], Roger M. Samelson[9], and Rebecca A. Woodgate[10]

9.1 Introduction

Observations have revealed persistent flows of relatively low salinity from the Pacific to the Arctic and from the Arctic to the Atlantic (Melling 2000). It is customary to associate fluxes of fresh-water with these flows of brine, as follows: the fresh-water flux is the volume of fresh water that must be combined with a volume of reference-salinity water to yield the volume of seawater of the salinity observed. As with sensible heat flux, the choice of reference is arbitrary, but the value 34.8 is often used in discussions of the Arctic. This value is an estimate of the mean salinity of the Arctic Ocean by Aagaard and Carmack (1989) for a time period and averaging domain that were not specified. Because the salinity of seawater flowing across the shallow Bering, Chukchi and Canadian Polar shelves is typically lower than 34.8, these flows transport fresh-water from the Pacific to the Atlantic Ocean.

---

[1] Fisheries and Oceans Canada, Institute of Ocean Sciences, Box 6000 Sidney BC Canada V8S 3J2

[2] Environment Canada, Meteorological Service of Canada, 4905 Dufferin St. Downsview ON Canada M3H 5T4

[3] College of Ocean and Atmospheric Science, Oregon State University, Corvallis, OR 97331-5503, USA

[4] Fisheries and Oceans Canada, Bedford Institute of Oceanography, Box 1006 Dartmouth NS Canada B2Y 4A2

[5] Applied Physics Laboratory, University of Washington, 1013 NE 40th St. Seattle WA 98105, USA

[6] College of Marine Studies, University of Delaware, 44112 Robinson Hall, Newark DE 19716, USA

[7] Fisheries and Oceans Canada, Bedford Institute of Oceanography, Box 1006 Dartmouth NS. Canada B2Y 4A2

[8] Fisheries and Oceans Canada, Bedford Institute of Oceanography, Box 1006 Dartmouth NS Canada B2Y 4A2

[9] College of Ocean and Atmospheric Science, Oregon State University, Corvallis OR 97331-5503, USA

[10] Applied Physics Laboratory, University of Washington, 1013 NE 40th St. Seattle WA 98105, USA

The transfer of waters from the Pacific to the Atlantic has been attributed to the higher sea level of the Pacific (Stigebrandt 1984; Wijffels et al. 1992), which is in turn the steric manifestation of lower salinity in the North Pacific relative to the North Atlantic. Steele and Ermold (2007) have examined the steric anomaly field derived from hydrographic data in the North Pacific Arctic and North Atlantic Oceans, 1950–2000. Their calculations, referenced to 1,000-db, suggest that Pacific Sea level at 55° N (zonal mean) is 0.55 m higher than Arctic sea level at 75° N (Beaufort gyre) and 1 m higher than Atlantic sea level at 85° N (Greenland Sea).

The magnitude and variability of volume and fresh-water fluxes through Bering Strait and the Canadian Archipelago are not well known (Melling 2000). The earliest geostrophic calculations of volume fluxes, based on bottle casts in the 1960s, were frequently cited until the late 1990s. At this time, volume flux had not been measured with established accuracy in any channel. The few estimates of fresh-water flux were inadequate, being products of long-term averages (volume flux and fresh-water anomaly) rather than averages of products. The wide variation (32–34: Aagaard and Carmack 1989; Prinsenberg and Bennett 1987; Sadler 1976) in the assumed salinity of through-flow for these estimates is indicative of their large uncertainty, equivalent to a factor of 3 in fresh-water flux. Geostrophic calculations were not referenced to measured currents until the 1980s (Prinsenberg and Bennett 1987; Fissel et al. 1988).

There were good reasons for the inadequate state of knowledge less than a decade ago (Melling 2000). One was political, the bisection of Bering Strait by a national jurisdictional boundary. Another was a geographic peculiarity, namely the proximity of the magnetic pole (80° N 105° W) to the Canadian Archipelago, which renders the geomagnetic field unreliable as a direction reference. Others were logistical – remoteness, harsh climate, persistent pack ice – or technical challenges to observation – hazard from moving sea ice and icebergs. Some arose from the nature of the flows themselves, such as small scales of motion, re-circulation and dramatic annual and inter-annual variability. Constraints on numerical simulation included computing capacity and deficient bathymetric and hydrographic information.

Lack of observations, attributable in large part to deficient technology, had been the principal impediment to scientific progress for many years. However by the late 1990s, improved technological capability provided the incentive for a renewed initiative to measure Pacific–Arctic through-flow. Doppler sonar, which offered the potential to measure near-surface current from a safe depth provided that zooplankton scatterers were sufficiently abundant, had been proven effective for year-round use in Arctic waters (Melling et al. 1995). Developments in microprocessors had opened up possibilities for smart instruments and new low-power electronics promised much longer operating intervals for sub-sea instruments. New all-weather microwave sensors offered higher resolution for ice reconnaissance, and developments in software permitted the automated tracking of pack drift and deformation.

Some technological challenges remain: how to measure current and salinity in the zone of extreme hazard from drifting ice, the upper 30 m of the ocean where much of the fresh-water flux occurs; how to recover moored instruments from remote areas of the Canadian Archipelago that are rarely free of ice; how to build affordable arrays that resolve the baroclinic scale of motion (5 km) across wide

channels; how to measure the direction of current in the vicinity of the geomagnetic pole in the Canadian Arctic. Moreover, numerical simulation of circulation in geography of such complexity is in its infancy.

The ultimate objective of ASOF is understanding the Arctic branch of the global hydrologic cycle. Moreover, useful predictions of changing climate are dependent on realistic parameterization of the relevant oceanic processes for computer simulation. For this we need greatly improved understanding of the forcing and controls on oceanic fresh-water flux from Pacific to Arctic to Atlantic. Specific topics where we need improved theoretical knowledge are:

- Sea-level differences between Pacific, Arctic and Atlantic basins
- Through-flow forcing by inter-basin differences in sea level
- Through-flow forcing by wind and atmospheric pressure
- Dynamics of rotating flow through channels of realistic geometry
- Boundary stress at the seafloor and the ice canopy in tidal channels
- Buoyant boundary flow through a network of 'wide' interconnected channels
- Lagrangian aspects of mixing in channels

A unique aspect of Arctic channel flows is their seasonally varying canopy of pack ice. When the pack is comprised of small floes at moderate concentration, its main impact is on the stress exerted by wind on the ocean surface. However, when large thick floes are present at high concentration, they can jam within the channel (Sodhi 1977; Pritchard et al. 1979). As ice drift continues downstream of the blockage, an arch becomes evident marking the boundary between open water and fast ice. In addition to its obvious effect of stopping ice flux through straits, a fast-ice canopy reduces the oceanic flux by imposing additional drag at the upper boundary of the flow. Ice cover introduces several additional theoretical challenges:

- Dynamics of pack-ice flow through channels of realistic geometry
- Stable ice-arch formation in channels of realistic geometry
- Dynamical interactions between the flows of water and of pack ice in channels

In the context of climate change, it is interesting to compare the mobility of pack ice that populates the three principal exits routes of ice from the Arctic Ocean. Ice within the channels of the Canadian Archipelago is fast for 8–10 months of the year, when it completely blocks ice export from the Arctic. Within Fram Strait, the pack ice is never fast and there is export of fresh-water to the Atlantic as ice year-round. Ice in Nares Strait flickers between these extremes, sometimes providing an export route year-round and in some years blocking ice drift from December through July.

If the Canadian Arctic channels were simply plumbing, carrying water without modification from ocean to ocean, Davis Strait would offer the appeal of metering the total through-flow on a single section, although its great width (2.5 times the total of other gateways) and cross-section (five times the total) would present challenge. However, the vastness of the Bering and Chukchi Seas and of the Canadian polar shelf precludes their simplification to conduits that convey water without modification from the Arctic to the Atlantic. At least three check points are needed to develop a useful understanding the Arctic's role in the global hydrologic cycle: at entry to

Arctic and exit from Pacific, at outflow from the Arctic Ocean over the Canadian polar shelf and at exit from the Arctic and entry to the Atlantic.

For practical reasons, observations have been focused at constrictions along the pathways joining the North Pacific to the Atlantic through the Arctic. These are circled and labeled on the map in Fig. 9.1. All inflow from the Pacific Ocean passes through Bering Strait, a short wide (85 km, with two islands obstructing about 9 km) channel separating the Bering and Chukchi Seas; the greatest depth in the strait is 60 m, but there is a sill of 47-m depth about 200 km to the southwest. In contrast, the channels of the Canadian Archipelago are much longer than they are wide. The Archipelago occupies slightly less than half of the Canadian polar continental shelf, which at 2.9×10^6 km^2 represents almost a quarter of the Arctic Ocean area (13.2×10^6 km^2). Its many channels have been deepened by glacial action to form network of basins as deep as 600 m, separated by sills. Deep (365–440 m) sills at the western margin of the continental shelf are the first impediment to inflow from the Canada Basin, but the shallowest sills are in the central and southern parts. For flux measurement, there is an optimal set of relatively narrow, shallow straits
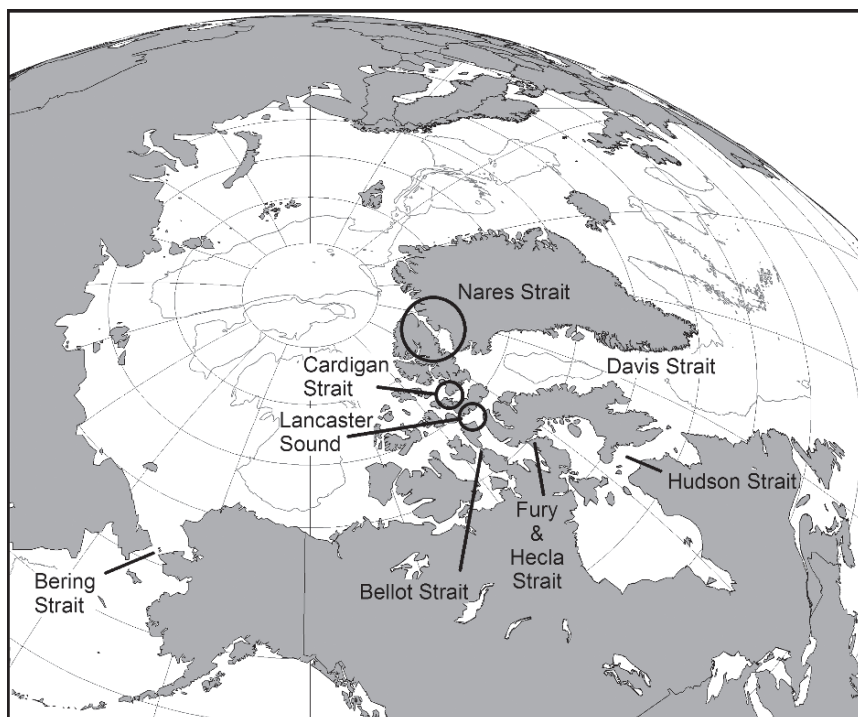
Fig. 9.1 The Arctic Ocean with focus on the North American shelves. The gateways for Pacific Arctic through-flow are indicated. To reduce congestion, the Lancaster Sound tag has been used as a single identifier of Barrow Strait to the west and Wellington Channel to the north-west; the Cardigan Strait tag also represents nearby Hell Gate. The 1,000-m isobath is plotted to delineate the continental shelves, ridges and ocean basins

through which all flow must pass: Bellot Strait, Barrow Strait (east of Peel Sound), Wellington Channel, Cardigan Strait, Hell Gate and Kennedy Channel. Among these, Bellot Strait is probably of little importance because it has such a small cross-section at the sill (less than 24 m deep, 1.9 km wide).

Although the net flux of volume is towards the Atlantic, water is exchanged in both directions between Baffin Bay and the Arctic Ocean. It is modified by mixing, freezing and melting during the months spent over the shelf and may ultimately be re-circulated back to its source. In contrast to Bering Strait, where re-circulation is usually dependent upon temporal reversals in flow direction, that within the Canadian Arctic is implicit in the spatial pattern of the circulation and the strength of tidally forced mixing and entrainment. The important net fluxes of volume and fresh-water must, therefore, be calculated as the differences between the much larger fluxes in opposing directions through adjacent parts of the cross-section.

Understanding of the fresh-water flux through the North American Arctic is presently inadequate to permit prediction of its sensitivity to climate change. The science is at the stage of basic research, during which monitoring of through-flow to detect variation and change must be a stand-in for simulation and forecast. However, the infrastructure needed to measure fluxes at all gateways for through-flow is not sustainable in the long run. A more tractable observing system will likely involve the integration of data from a few points of prolonged observation and realistic simulations of through-flow by numerical ocean circulation models; these must be driven in the greater part by observations that are readily available. We anticipate an opportunity to relax observational diligence when a capability in numerical simulation of Pacific Arctic through-flow has been demonstrated.

This chapter starts in a geographic progression from west to east around the North American continent, exploring recent advances in the empirical knowledge of volume and fresh-water through-flows via Bering Strait into the Arctic and via the gateways of the Canadian Archipelago that open into Baffin Bay. In order from southwest to northeast these are Lancaster Sound, Cardigan Strait, Hell Gate and Nares Strait. The subsequent sections review progress in relation to three issues common to all gateways – numerical simulation of Canadian Arctic through-flow, sea-ice budget for the Canadian polar shelf, mesoscale orographic influence on wind forcing in Arctic sea straits and trace chemicals in seawater as indicators of the sources, mixing and transit times for Pacific–Arctic through-flow. The final geographically oriented section examines Davis Strait, where Arctic fresh water is delivered to the convective gyre of the Labrador Sea. A closing section takes stock of our progress in the Arctic sub-Arctic Ocean fluxes study and identifies the issues that impede our understanding of fresh-water flows and dynamics in the North American Arctic.

9.2 Pacific Arctic Inflow via Bering Strait

Bering Strait is the only gateway between the Pacific and the Arctic Oceans. On an annual average, the flow through the strait is northwards; it is likely a consequence of decreasing sea level from south to north, Pacific to Arctic. The steric anomaly

computed from hydrographic data support this interpretation, but the difference in geopotential across the Bering and Chukchi shelves has yet to be measured. Regional winds, which are southward on average, oppose flow into the Arctic (Coachman and Aagaard 1966, 1981; Woodgate et al. 2005b). Melling (2000) provides an overview of early studies.

Since 1990, measurements of temperature, salinity, current have been made in Bering Strait almost continuously at one site and sometimes at two or three sites simultaneously (Fig. 9.2; Roach et al. 1995; Woodgate et al. 2005a). Instruments have been positioned near the seabed to avoid damage from ice keels that can extend to 20-m depth. Before 2000, hydrographic sections were measured only sporadically and only in summer (Coachman et al. 1975). Since 2000, sections have been measured every year, but again only in summer. Snapshots of flow structure at high spatial resolution have been measured several times by ship-mounted ADCP. Such detailed views, though transient, are essential for justifying (or otherwise) the validity of flux estimates based on long-term data acquired at only one or two points across the section.

The observations since 1990 have revealed an average annual flux of volume through Bering Strait of about 0.8 Sv towards the Arctic (Coachman and Aagaard 1981; Roach et al. 1995; Woodgate et al. 2005a). Higher estimates from earlier times (e.g. 1.2 Sv in the 1950s: Mosby 1962) likely reflect the greater uncertainty of measurement using the technology and methods then available. The best estimate
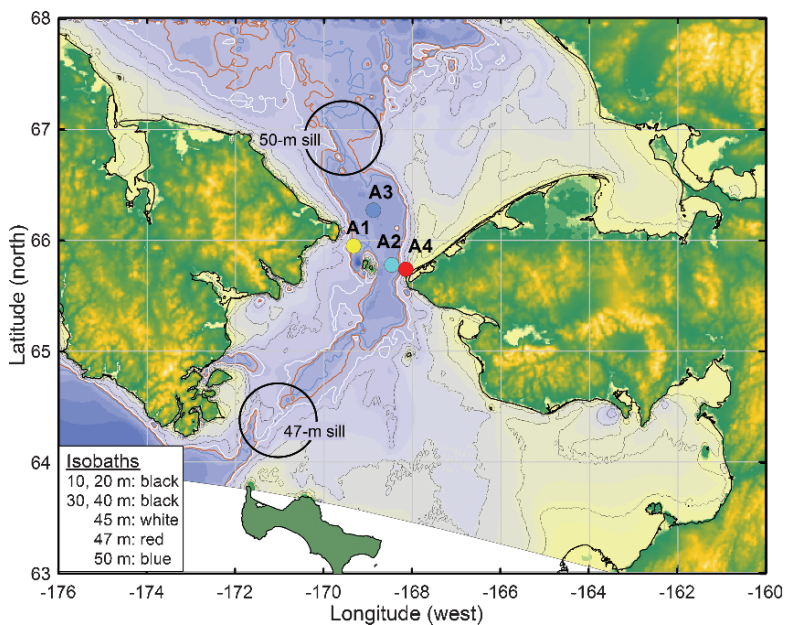
Fig. 9.2 Bering Strait showing the locations of moorings for determining through-flow (coloured discs). The sills limiting through-flow from the Pacific Ocean are circled

of the fresh-water flux through Bering Strait, circa 1990, was 1,670 km^3/year (53 mSv) relative to 34.8-salinity, calculated by Aagaard and Carmack (1989) for their review of Arctic Ocean fresh-water; these authors used Mosby's value for the average volume flux and an assumed annual average salinity of 32.5 (based mainly on hydrographic measurements in summer during the 1960s and 1970s).

Simultaneous observations at several sites during the last 5 years have provided some new information on the structure and variability of the Bering Strait through-flow (Woodgate and Aagaard 2005). In particular, an ADCP moored near the Alaskan coast has revealed the important contribution, previously unacknowledged, of the low salinity Alaskan Coastal Current (Paquette and Bourke 1974; Ahlnäs and Garrison 1984) to the fresh-water flux through Bering Strait. Woodgate and Aagaard (2005) now estimate that this stream contributes 220–450 km^3/year (7–14 mSv) to the fresh-water flux. Moreover, a previously ignored decrease in salinity towards the surface in mid strait is responsible for a second fresh-water flux increment of 350 km^3/year (11 mSv). These new contributions increase the flux of fresh-water via Bering Strait by about 50%, to 2,500 ± 300 km^3/year (80 ± 10 mSv), equivalent to three quarters of the fresh-water inflow to the Arctic Ocean via rivers. The contribution from ice flux through Bering Strait remains unknown.

Annual average values conceal strong annual cycles in fluxes through Bering Strait. Monthly mean volume flux is typically highest in summer (1.3 Sv in June), when the prevailing north wind of this region is weakest (Roach et al. 1995; Woodgate et al. 2005a). The flux decreases in winter under the influence of stronger north winds and reaches a minimum of about 0.4 Sv in January. A concurrent increase in salinity contributes to a much reduced northward flux of fresh water in winter; the minimum is 100 km^3/month (38 mSv) in January (Serreze et al. 2006). A lower near-bottom salinity, the presence of the Alaskan Coastal Current (April–December) and stronger salt stratification throughout the Strait (salinity decreases by 0.5–1 from seabed to surface: Woodgate et al. 2005a) act in concert with the stronger northward current to increase the fresh-water flux in summer; the maximum is 300–400 km^3/month (115–150 mSv) in June.

A model operating at 9-km resolution has been successful in simulating a seasonal cycle although it is weaker and lagged by 2 months relative to observations: the modelled fresh-water flux reaches a maximum at 220 km^3/month in July or August and a minimum at 80 km^3/month in March or April (Clement et al. 2005). The discrepancy between the model and observations has been attributed to the model's lower northward volume flux (only 0.65 Sv) and its poor resolution of the Alaskan Coastal Current. On the other hand, the observational basis for flux estimates within the Alaskan Coastal Current is also meagre. Prolonged measurements of the flow and stratification of the Alaskan Coastal Current (now viable using new technology) are needed to reduce uncertainty in this component of the Bering Strait through-flow.

Although the seasonal cycles in fresh-water flux through Bering Strait is strongly linked to that in volume, the former is also independently forced by seasonal sources of fresh water to the south, the Yukon River for example. The maximum monthly outflow of the Yukon River is only 40 km^3 and the total outflow of all rivers

into the Bering Sea is 300 km³ each year (http://nwis.waterdata.usgs.gov/usa/nwis/
discharge; Lammers et al. 2001). Therefore, other sources of fresh water must con-
tribute to the 220–450 km³/year that the Alaska Coastal Current carries through
Bering Strait. The fresh-water influx from the Gulf of Alaska to the Bering Sea
(500 km³/year: Weingartner et al. 2005) is large enough to be the unrecognized con-
tributor, but it is difficult to reconcile the 2-month lag for transit from the Aleutians
to Bering Strait with observed seasonal variation in the Bering Strait through-flow.

Over periods of years, the variation of fresh-water flux is influenced by variations
in both volume flux and in seawater salinity (Fig. 9.3: Woodgate et al. 2006). The
highest annual mean volume flux occurred in 1994 (1 Sv), whereas the annual mean
salinity at the seabed was highest in 1991 (32.8). Since 1998, when a better obser-
vational array was established, the fresh-water flux has ranged from 2,000 km³/year
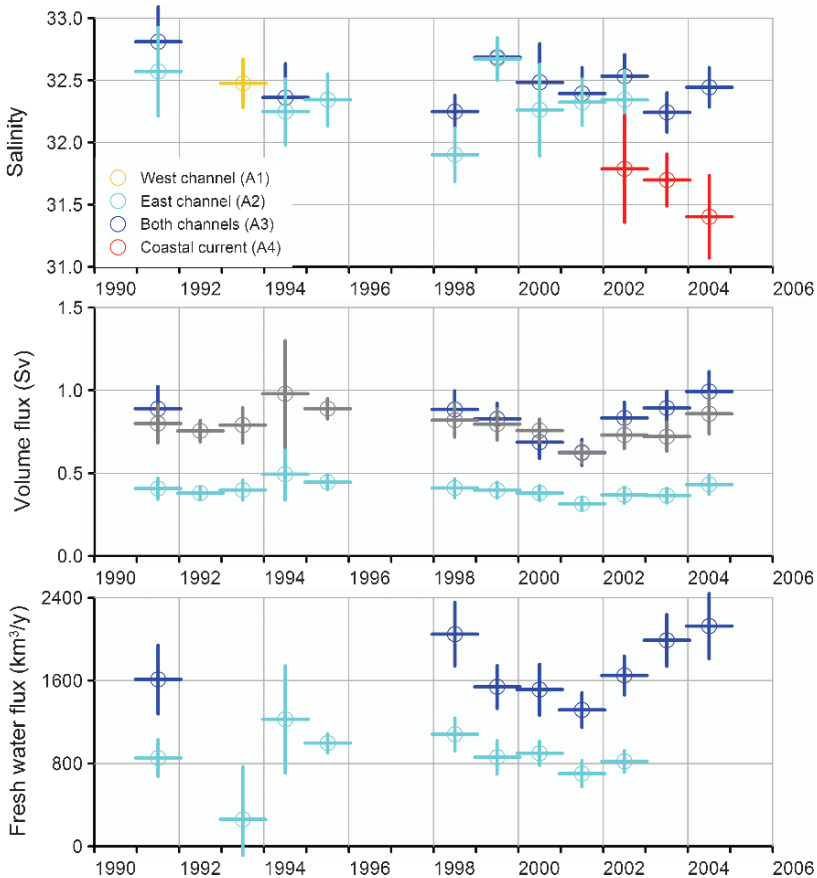
Fig. 9.3 Annual mean values of near-bottom salinity, volume flux and fresh-water flux derived from
Bering Strait moorings as indicated by colouration. For flux estimates, blue (from A3) represents the
entire strait, cyan (from A2) only the eastern channel and grey the entire strait, estimated from A2
only. Dashed lines indicate uncertainty in the means (Adapted from Woodgate et al. 2006)

Table 9.1 Fluxes of volume and fresh water through Bering Strait. Contributions of the Alaskan Coastal Current to the fresh-water flux have been included except in the estimate for inter-annual variation, for which there are insufficient data

	Volume (Sv)	Fresh Water (mSv)
Annual minimum (January)	0.4	38
Annual maximum (June)	1.3	115–150
Long-term mean	0.8	80
Inter-annual variation	±0.2	±10

(63 mSv) in 1998, to 1,400 km³/year (44 mSv) in 2001 and back to 2,000 km³/year in 2004. The 43% increase between 2001 and 2004 equals almost one quarter of the total annual inflow to the Arctic from rivers. Weakened north winds and consequent increased volume flux (0.7–1.0 Sv) explains 80% of the increase in fresh-water flux at this time (Woodgate et al. 2006). Clearly atmospheric variability in the Bering–Chukchi region has important influence on fluctuations in the Arctic fresh-water budget.

Current best estimates of fluxes through Bering Strait are summarized in Table 9.1. In this table, and in the preceding paragraph, the magnitude of inter-annual variation in fresh-water flux (1,400–2,000 km³/year) does not include the fresh-water transported within the Alaskan Coastal Current and within the low-salinity surface layer, because such observations were initiated only recently. Investigators now suggest that these components are likely more than one third of the total.

New autonomous instruments (notably IceCAT, an upper-layer sensor in a trawl-resistant housing that transfers data to a recorder at safe depth) may provide the means for year-round measurement of the important fresh-water flux near the ocean surface where risk from storm waves and ice-ridge keels is high. Information from sensors on Earth satellites can also be valuable. For example thermal sensors have been used to delineate the northward flow of warm (and river-freshened) seawater in the coastal current, and radar altimeters have provided estimates of the atmospherically variability in the flux through Bering Strait via direct measurements of sea level on assumption of geostrophy (Cherniawsky et al. 2005).

International politics have been an impediment to flux measurement in Bering Strait, which is split between the Exclusive Economic Zones of the United States and Russia. Since 2004, a joint US–Russian scientific programme RUSALCA (Russian–American Long-term Census of the Arctic), lead in the USA by NOAA, has facilitated the installation of instruments on moorings to measure fluxes in the western channel of the Bering Strait.

## 9.3   Flux and Variability in Lancaster Sound

Lancaster Sound is the southernmost of the three principal constrictions to flow across the Canadian polar shelf between the Arctic Ocean and Baffin Bay (Fig. 9.1). It ranks second to Bering Strait in the duration of ocean flux measurements. Current

meters were moored in Barrow Strait, to the west of Lancaster Sound, for 4 years during the early 1980s, providing data for the calculation of volume and fresh-water fluxes, subject to limitations of the technology of the time (Prinsenberg and Bennet 1987; Fissel et al. 1988). An array of new generation instruments was established in 1998 about 100 km further east (western Lancaster Sound) with intent to measure the combined outflows of seawater from Barrow Strait to the west and Wellington Channel to the north-west. Lancaster Sound is 68 km wide at this location and has a maximum depth of 285 m (Fig. 9.4). The array continues to evolve with the development and proving of new technology for this challenging application.

The location in Lancaster Sound is ice covered for as long as 10 months every year and typically lies beneath fast ice for half this time. It is well positioned logistically because it can be conveniently serviced in August via the icebreakers of the Canadian Coast Guard that routinely operate near Resolute Bay. Moorings have been recovered and redeployed annually and a modest hydrographic survey has been completed via CTD, with water sampling for analysis of geochemical tracers.

Arctic surface water occupies the upper part of the instrumented section. In summer, the coldest water ($-1.7\,°C$, 32.8–33.0 salinity) is at 50–100 m depth, a remnant of winter (Prinsenberg and Hamilton 2005). Above this layer lies less dense surface water formed by addition of ice melt-water and runoff and by warming through insolation. The lightest water is organized into buoyancy boundary currents that flow in opposite directions along the northern and southern shores. The temperature and salinity increase with depth below the remnant winter waters. Some of this deeper water has arrived from the north and west (Melling et al. 1984; de Lange Boom et al. 1987) but the warmest and most saline is derived from the West Greenland Current in Baffin Bay to the east.

Because the keels of ice ridges threaten near-surface instruments, moorings have not extended above 30-m depth. For this reason, the array incorporates an ICYCLER in addition to the familiar instruments for measuring current, temperature and salinity. The ICYCLER periodically deploys a buoyant temperature-conductivity module
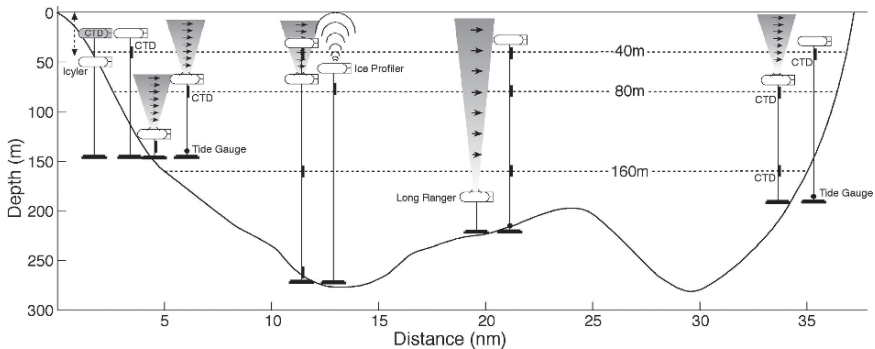
Fig. 9.4 The expanded array of moorings in Lancaster Sound used for through-flow measurements during 2005–2006. The instruments were concentrated near the southern shore (left of figure) in order to detect the buoyancy boundary current which carries much of the Arctic through-flow

upwards to the ice, measuring fresh-water and heat in the hazardous part of the water column. A comparison has revealed that a fresh-water inventory calculated using ICYCLER data is 20% larger during June to October than that inferred by extrapolation from data recorded at a fixed depth of 30 m. Since flow speed also increases towards the surface, the impact of accurate surface data on computed fresh-water flux is quite dramatic. During the cold part of the year in Lancaster Sound, when the surface mixed layer is deeper than 30 m, a sensor at 30-m depth provides a better measure of the near-surface fresh-water inventory. Since 2004, the array has also included ice-profiling sonar (IPS). Pack-ice draft data from this instrument in combination with ice tracking by the ADCP provide the component of fresh-water flux moved by pack-ice (e.g. Melling and Riedel 1996).

Reliance on the magnetic compass for a reference direction is standard practice in oceanography. However in western Lancaster Sound only 800 km from the north magnetic pole, the horizontal component of the Earth's field is less than 2,500 nT, the inclination of field lines is almost vertical (87.6°) and the magnetic declination is significantly perturbed by ionospheric effects over a range of time scales. To use a geomagnetic reference under such conditions, instrument orientation must be measured using a precise three-axis flux gate compass and the instantaneous geomagnetic vector must be monitored. Fortuitously for installations in Lancaster Sound, there is a geomagnetic observatory in nearby Resolute Bay. Details are provided by Prinsenberg and Hamilton (2005).

Based on a hydrographic section measured in August 1998, geostrophic calculations revealed an eastward current that extended across two thirds of the sound with highest speed at the surface near the southern shore (Prinsenberg and Hamilton 2005). There was weak westward flow at depth on the northern side. Subsequent study has shown that flow through the northern third of the section is quite variable and contributes little to net flux on a long-term average. In recognition of this apparent broad structure to the flow, the array of moored instruments provides observations of current, temperature and salinity at only 2–4 positions across the section.

In computing flux, it has been assumed that data from each location and depth represent average conditions across a specified sub-area of the cross-section, so that flux is the sum of area-weighted data. The selection of sub-sectional areas was guided by data from an expanded array of four sites in place during 2001–2004. This array provided the usual observations at sites in the coastal boundary currents near the southern and northern shores, and additional observations of near-surface (0–60 m) current at the quarter and half-way points from the southern shore (Fig. 9.4). Figure 9.5 displays the average of currents measured at 10, 30 and 50 m as weekly averages for three sites at 15-km spacing in the southern half of the section. At times, most often during November through May, upper ocean flow was similar at all three sites. However during the summer the shear across the channel was large; the speed at the southernmost mooring was almost twice the average value for the 3 sites. A seasonally varying weighting of data from the southernmost mooring has therefore been used in calculating fluxes at times when only two sites were established.
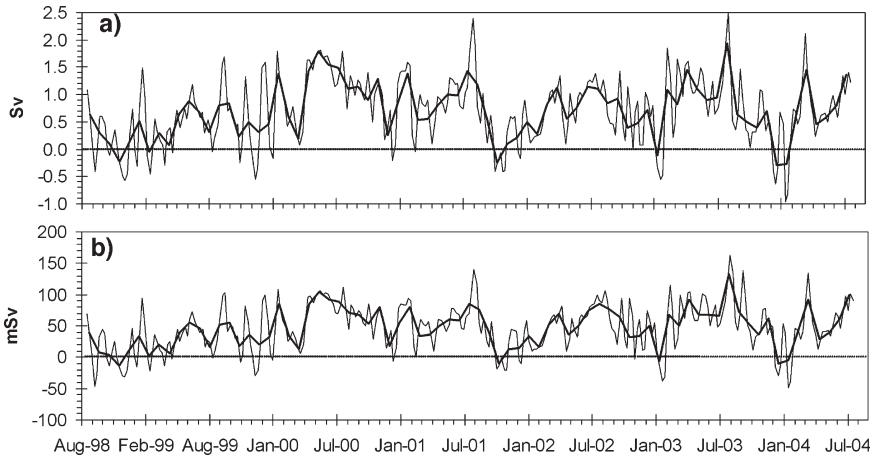
Estimated fluxes through Lancaster Sound are listed in Table 9.2 and plotted in Fig. 9.6; the reference value for fresh-water is 34.8. Volume flux has a 6-year mean
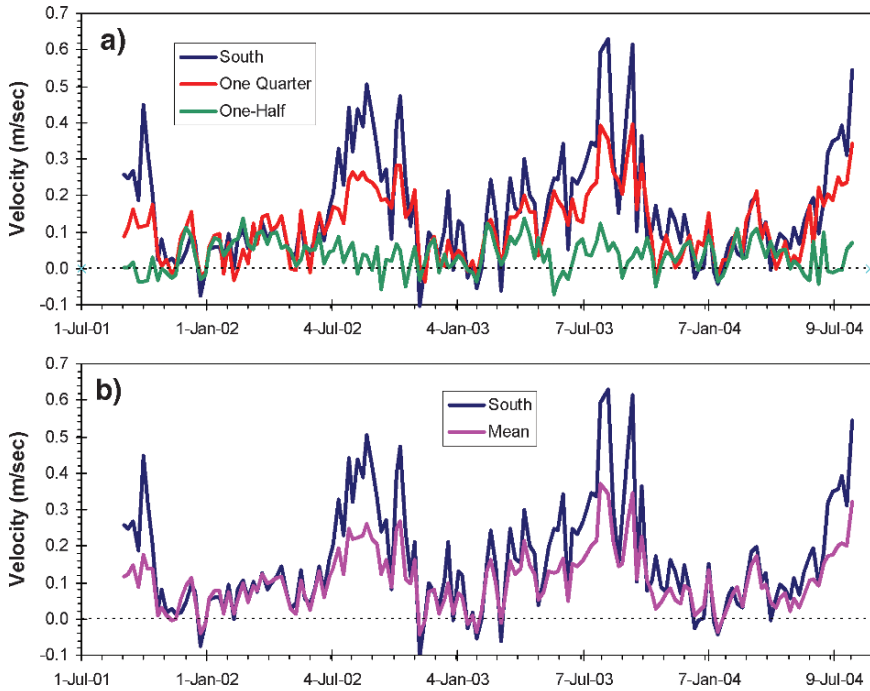
Fig. 9.5 Upper panel: The average value of currents measured at 10, 30 and 50 m for three locations in the southern half of Lancaster Sound, labelled by fractional distance from the southern shore. Lower panel: Average of the three curves in the upper panel compared with the time series from the southernmost site. All values are week-long averages

Table 9.2 Fluxes of volume and fresh-water through Lancaster Sound as seasonal and annual averages for August 1998 to August 2004. The reference salinity for fresh-water flux is 34.8. Arctic exports have positive value

|		Fall	Winter	Spring	Summer	Year
1998–1999	Volume (Sv)	−0.01	0.37	0.48	0.70	0.39
	Fresh-water (mSv)	**10**	**26**	**31**	**44**	**26**
1999–2000	Volume (Sv)	0.25	0.91	1.09	1.32	0.89
	Fresh-water (mSv)	**20**	**56**	**65**	**81**	**56**
2000–2001	Volume (Sv)	0.97	0.82	0.81	1.19	0.95
	Fresh-water (mSv)	**59**	**51**	**51**	**72**	**58**
2001–2002	Volume (Sv)	0.11	0.35	0.87	0.93	0.56
	Fresh-water (mSv)	**14**	**22**	**55**	**70**	**40**
2002–2003	Volume (Sv)	0.60	0.54	1.18	1.13	0.86
	Fresh-water (mSv)	**45**	**34**	**77**	**92**	**62**
2003–2004	Volume (Sv)	0.31	0.45	0.63	1.24	0.57
	Fresh-water (mSv)	**35**	**34**	**43**	**93**	**45**

Fig. 9.6 Time series of weekly and monthly averaged fluxes through western Lancaster Sound, August 1998–2004
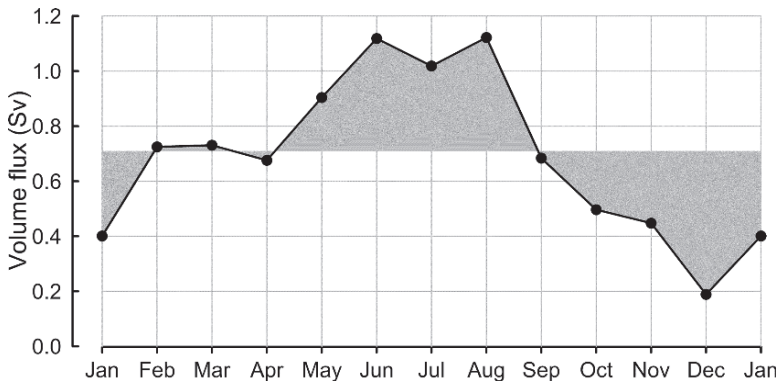
Fig. 9.7 Annual cycle in volume flux through western Lancaster Sound, as means for each month computed for the 6-year record of measurements, August 1998–2004

of 0.7 Sv, with yearly averages spanning a range of 0.4–1.0 Sv. There is a strong annual cycle (Fig. 9.7), ranging between low values in autumn and winter (0.2 Sv) and high values in summer (1.1 Sv). The fresh-water flux is typically about 1/15 of the volume flux – 6-year mean of 48 mSv (1,510 km³/year) – and has a similar seasonal cycle. The range of variation in annual means is 36 mSv (1,140 km³/year).

Atmospheric variability is one possible driver of flow variability in Lancaster Sound. Figure 9.8 displays an obvious co-variation of 12-month running averages of the NAO Index and of fresh-water flux through Lancaster Sound; the former has been delayed by 8 months. One possible linking mechanism is the oceanic response to the AO, mediated primarily via Ekman pumping and via lateral displacement of the Beaufort gyre. The associated cycle in the ocean circulation pattern has been
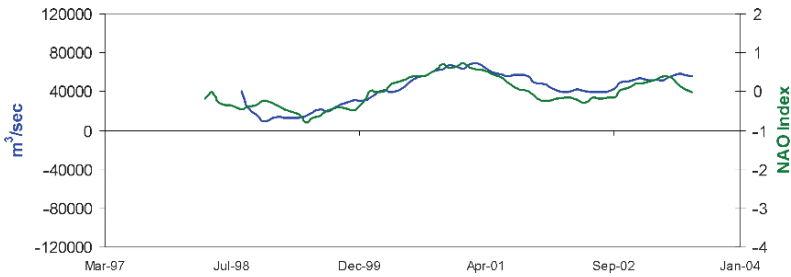
Fig. 9.8 12-month running averages of the fresh-water flux through Lancaster Sound and of the NAO index, with the latter delayed by 8 months

labelled the Arctic Ocean Oscillation (AOO) by Häkkinen and Proshutinsky (2004). Under this interpretation, the 8-month lag of the flow surge in Lancaster Sound could represent the spin-up time of the AOO. The possible role of the AOO in forcing Canadian Arctic through-flow is discussed further in the section on chemical tracers.

One goal of present study is the demonstration of a minimal array of moored instruments that could monitor fluxes through Lancaster Sound over the long term with help from numerical ocean models. The relative magnitudes of flows at three locations in the southern half of the section have already been discussed. The lower panel of Fig. 9.5 shows that the upper ocean flow 22 km from the southern shore was close to the average of values from all the three sites during a 3-year period of trial. This demonstration is the basis of a proposed flux-monitoring installation at this location: 300-kHz ADCP at 75 m to measure upper-ocean current and ice drift, bottom-mounted 75-kHz ADCP (with pressure sensor) to measure deep current, IPS at 50 m to measure ice draft, temperature-conductivity recorders at several depths below 50 m and an ICYCLER to determine profiles of temperature and salinity in the upper 50 m and a pressure gauge.

Ultimately, if Canadian Arctic through-flow is found to be predominately barotropic, then precise, geodetically referenced sea-level stations around the Canadian Archipelago could provide the information needed by numerical models to determine the oceanic fluxes.

9.4   Structure of Flow in Hell Gate/Cardigan Strait

In 1998, Fisheries and Oceans Canada began a study of current in Cardigan Strait with two goals that are fundamental to the successful measurement of fluxes through the Archipelago: (1) a reliable and cost-effective method of measuring current direction near the geomagnetic pole, and (2) a better knowledge of the spatial structure of Arctic channel flows. The latter information is essential to the design of sparse arrays of moored instruments for accurate measurement of oceanic through-flow.

Cardigan Strait had advantages as an experimental site. Because of its simple geometry and narrow width (8 km: Fig. 9.9), the through-flow could perhaps be resolved at the internal Rossby scale using a small number of moorings. Mixing by strong tidal currents (2 m/s) could be expected to weaken the density stratification and thereby to reduce the importance of the difficult-to-measure baroclinic component of flow. Moreover, strong tides provided a key to measuring current direction in the Canadian Arctic because tidal ellipses in a narrow strait are necessarily flat and aligned with the strait's axis. Nearby Hell Gate was an experimental control with half the width and contrasting 'dog-leg' geometry.

The study in Cardigan Strait was planned in phases of 2-year duration. The objective of the first phase, 1998–2000, was evaluation of a new torsionally rigid mooring for ADCPs; that of the second was investigation of co-variability between flows in Cardigan Strait and in Hell Gate; that of the third was a look at the cross-sectional structure of flow within Cardigan Strait. In response to presently ambiguous results, the third phase has been continued beyond 2005.

A unique mooring (Fig. 9.10) was designed to meet the special challenges of this environment. It was torsionally rigid to keep the ADCP on a fixed geographic heading throughout the deployment; a universal joint in the backbone allowed the mooring to stand upright regardless of seabed roughness and slope. The ADCP itself was mounted in gimbals to remain zenith-pointing during lay-over of the mooring in
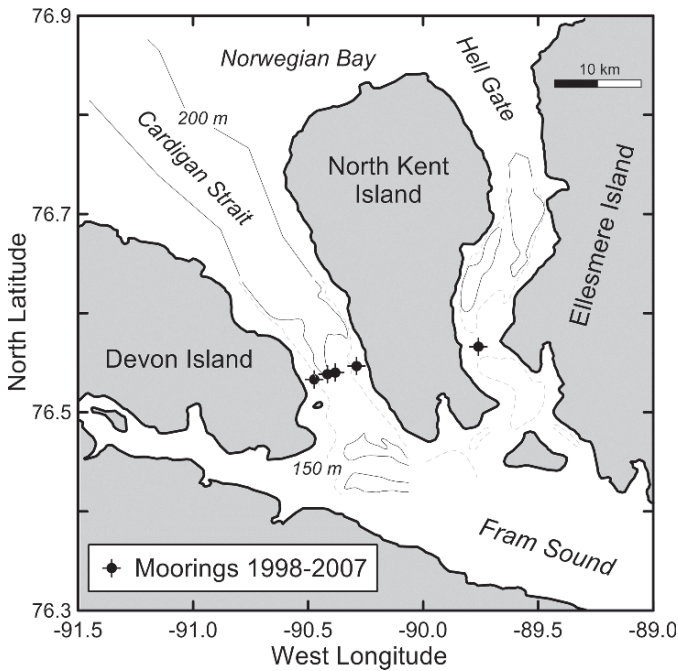
Fig. 9.9 Cardigan Strait and Hell Gate, showing the locations of moorings at the sills. The plotted 150 and 200-m isobaths are based on sparse soundings
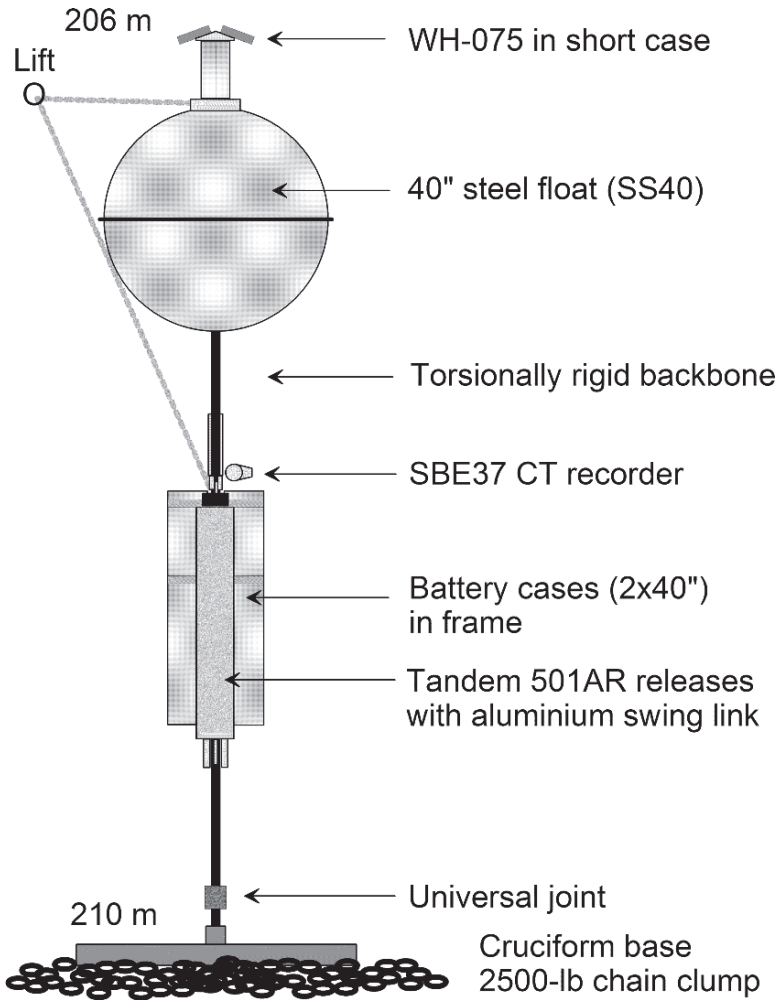
Fig. 9.10 Torsionally rigid mooring designed to address the various difficulties of measuring current in the Canadian Archipelago

strong current. The mooring rose only 3 m from the seafloor so as to minimize its sensitivity to the drag from current and its vulnerability to icebergs. The mooring was designed for free fall from the surface, enabling expeditious deployment in fast current and drifting ice; heavy chain arranged in loops as part of the deadweight anchor cushioned the shock of landing at 3 m/s.

Phase 1 provided proof of the value of the new mooring, which was over the side and deployed in 30 s, survived impact at the seabed and held the ADCP within ± 1° of upright in 2 m/s current and at constant heading for 2 years. The latter result justifies our reliance on a tidal-stream analysis of the recorded data to infer the ADCP's orientation. Current were measurable using backscattered sound to a range

of 100 m from early July to late January, but the effective range shrank to about 70 m for 3 months (April through June) when echoes were weak. The strong diurnal variation of echoes implies a biological explanation for the weak back-scatter in late winter. During the second phase, our trial with a 75-kHz ADCP was successful in providing current profiles to the surface (185-m range) in all seasons.

Annual mean currents at three locations across Cardigan Strait are shown in Fig. 9.11. Measurements were made on the western slope during August 1998–2000, on the central axis during August 2000–2005 and on the eastern slope during August 2002–2004. The observations reveal uniform current in the middle depth range and sheared flow near the seafloor and the surface. Benthic drag or hydraulics at the sill may influence the lower shear layer and baroclinicity or wind action the upper. The small year-to-year variation between 1998 and 1999 (western slope), between 2000 and 2001 (channel axis) and between 2002 and 2003 (both eastern slope and channel axis) initially prompted an interpretation that differences between sites were indications of a stable spatial structure for the flow. For example, the left and centre panels of the figure (data not synoptic) suggest a halving of speed in only 2.4 km; such a steep gradient raised doubt about fluxes calculated using data from a single location in this 8-km wide channel. However, on presumption that data from 1998–2002 provided a valid representation of a constant spatial structure in the flow, we estimated volume fluxes of 0.2 Sv and 0.1 Sv through Cardigan Strait and Hell Gate (2000–2002 data not shown), respectively.
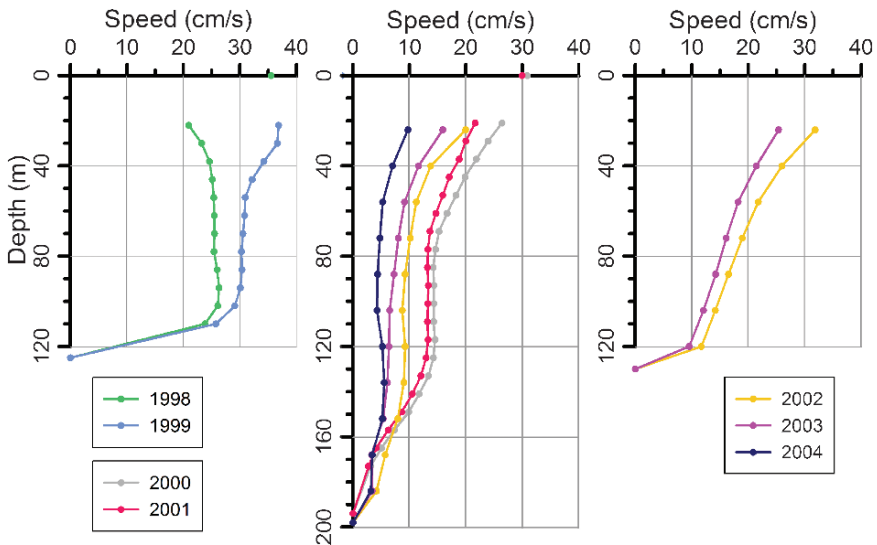

Fig. 9.11 Mean annual profiles of along-channel flow at three locations in Cardigan Strait, 1998–2005. An ADCP operated on the western slope during August 1998–2000 (left panel), on the central axis during August 2000–2005 (middle panel) and on the eastern slope during August 2002–2004 (right panel). Labels denote the starting August for the 12-month average. Positive values indicate flow towards Baffin Bay

Prolonged observation has provided new perspectives. Although the annual mean current at mid channel was much the same during 2000 and 2001 and during 2002 and 2003, the five annual values span a three-fold range. Clearly our early assumptions regarding a static cross-sectional variation and temporal constancy are invalid. Moreover, during 2002–2004, the mean (southward) current along the eastern slope of the Strait was about 50% stronger than the mean on the channel axis (Fig. 9.11); the flow along the western slope may also be stronger than on the axis. This pattern of cross-channel variation is consistent neither with a wall-bounded buoyancy current following the western slope nor with a frictionally controlled flow wherein current would be fastest at mid channel. We conclude that observations at more than two locations are required to calculate flux even in a channel as narrow as Cardigan Strait.

Results concerning seasonal variation in current are ambiguous; some data reveal an obvious annual cycle and some do not. One of the more definitive records, acquired on the eastern slope of Cardigan Strait during August 2002–2004, is plotted in Fig. 9.12. There is a strong Arctic outflow from January through September in both years (strongest in June), but during the autumn and early winter the average flow is weaker and the direction of flow reverses at times. This cycle is roughly in phase with that reported from Lancaster Sound as an average over 6 years of measurement. If this result survives more thorough analysis it will lend credence to a common forcing mechanism for both gateways, perhaps a seasonally varying pressure gradient from the Canada Basin to Baffin Bay that is weakest in the late autumn.

The difficulty of calculating volume flux through Cardigan Strait and Hell Gate has just been described. The challenge of calculating fresh-water flux as the covariance of flow velocity and salinity anomaly integrated across the channel section is even greater. The difficulty of delineating the cross-sectional variation of current is clear; measurement of the time-varying cross-section of salinity is even more problematic. Strong hydrodynamic drag (current up to 3 m/s in Hell Gate) effectively
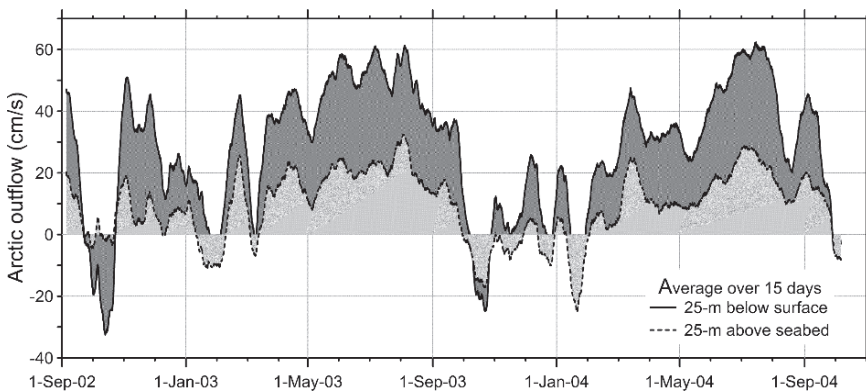
Fig. 9.12 Current at two levels on the eastern slope of Cardigan Strait, August 2002 to October 2004. Note the strong Arctic outflow during February through October. The record has been filtered to attenuate tides

precludes the use of conventional taut-line moorings to suspend temperature-conductivity recorders at fixed depths. Moreover, hydrographic fields are strongly forced by tidal flow over the sloping topography of the straits. At fixed depth near the seafloor, where temperature and salinity are presently being measured, the range in the value of these parameters over a tidal cycle is comparable to the range in values that might be measured via an instantaneous CTD cast from surface to seabed. This is perhaps indicative of fresh-water flux contributions from covariance at tidal frequency. An implied necessity to resolve variation of the salinity section at such high frequency cannot be met with present technology.

9.5   A Snapshot of Flux via Nares Strait

Because new long-term measurements of current and salinity from which fluxes in Nares Strait might be calculated have only recently been retrieved from the sea, the work of Sadler (1976) remains for now the standard reference. A 10-month record of current was acquired by an ADCP deployed near the Canadian shore in Smith Sound during the North Water Project in 1997–1998, but calculation of fluxes from single-point data in this wide sound is not defensible (Melling et al. 2001).

We do have an excellent set of observations acquired using ship-based ADCP during August 2003 which provide a detailed description of the cross-sectional structure of the through-flow. As discussed earlier, such information is essential to the use of data from widely spaced moorings in the calculation of fluxes and in the estimation of sampling error. It has also provided demonstrably accurate values, albeit short-term, of volume and fresh-water fluxes as benchmarks against which to assess values based on less well resolved measurements by moored instruments. The data from the high resolution surveys in Nares Strait and their significance for ocean-flux measurement using moored instruments are the subjects of this section.

LeBlond (1980) proposed that the generally cyclonic circulation of icebergs across the mouth of Lancaster Sound was a manifestation of buoyancy concentrated in narrow boundary currents of low salinity. Direct observations of these currents revealed an approximately geostrophic balance of flow and cross-channel pressure gradient (Prinsenberg and Bennett 1987; Sanderson 1987) on a 10-km scale comparable to the local internal Rossby radius of deformation.

In August 2003, a team on USCG Healy completed simultaneous surveys of current and salinity in Nares Strait. Flow data were acquired at high resolution using vessel-mounted acoustic Doppler current profiler (ADCP) and conventional hydrographic casts provided temperature and salinity (and therefore density) at 5-km spacing on selected sections. A notable feature of the salinity and density sections was the spreading of isopycnals at about 130-m depth within 10-km of Ellesmere Island (Münchow et al. 2006): isopycnals above this depth sloped upward toward the coast whereas those below it sloped downward. Such hydrographic structure is indicative of a sub-surface baroclinic jet hugging the western side of the channel. A weaker counter-flow of similar width was measured near the Greenland coast.

Healy's ADCP used a 75-kHz, hull-mounted, phased array. Echoes received at 2-s intervals were processed to yield a vertical profile of velocity relative to the ship. The ship's motion was derived from an independent bottom-tracking pulse (or via high precision GPS tracking) as described by Münchow et al. (2006). Because sonar beams were directed obliquely downwards, velocity could not be measured in the lowest 15% of the water column where there is interference from the seabed. Also, there are no data for the uppermost 25 m because the hull-mounted transducer was 8 m below the surface, because signals from the first 10 m of range were obscured by ring-down of the transmitter and because the sonar pulse averaged flow over 15 m increments in range.

Measured current was the sum of components at tidal and lower frequencies which vary with the position of the ship and with the time of measurement. Sub-tidal current was masked in each instantaneous measurement by tidal current which was generally much larger. However, because the tide is predictable in space and time (Padman and Erofeeva 2004) its contribution can be removed from each observation via collective analysis of the observations from all places and times. We fitted oscillations at tidal frequencies to velocities measured separately at different times for each depth of interest; this approach allowed realistic vertical variations in tidal current with friction and density stratification.

The continuous measurements of current from the slowly moving ship easily resolved flow features on the scale of the internal Rossby radius. The along-channel flow at sub-tidal frequency was observed to be spatially coherent with a Rossby number of 0.13, indicating near-geostrophic balance. Approximately one third of the total volume flux was associated with cross-channel slope of the sea surface (barotropic mode) and two thirds with across-channel slope of isopycnal surfaces (baroclinic mode).

One section at 80.5° N (Fig. 9.13) was measured repeatedly over several tidal cycles. The sub-tidal flow was southward with much of the flux in the western half of the channel above 200-m depth. The principal feature was a sub-surface jet that reached a maximum speed of 0.3 m/s about 12 km from the Ellesmere coast. The calculated net flux of seawater averaged over several days of observation was 0.8 ± 0.3 Sv towards Baffin Bay. The southward net flux of fresh water was 25 ± 12 mSv (790 km^3/year). These values are dependent upon assumption of current speed within the upper 30 m of the water column, which could not be measured. The fresh-water flux is particularly sensitive to the assumption because the low salinity of surface water strongly weights the current in this layer upon integration. The quoted confidence limit for fresh-water flux is the difference between a lower bound that neglects flux above the shallowest depth of measurement and an upper bound for which current was assumed uniform in the top layer and equal to the average flow in the shallowest two levels of measurement (18–48 m).

A second section with good observational coverage was completed in Robeson Channel at the northern end of Nares Strait. This survey encompassed the locations where current was measured for 6 weeks in the spring of 1971. Data from three sites at this time provided the often cited 0.6 ± 0.1 Sv through-flow value for Nares Strait (Sadler 1976); the attribution of more than 50% of the calculated flux to the record
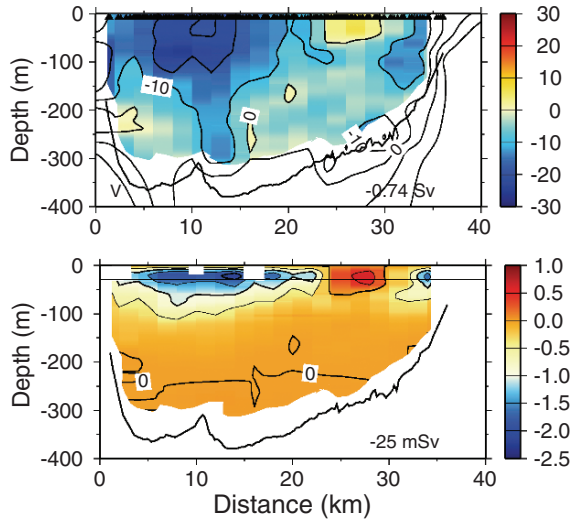
Fig. 9.13 Distribution of volume flux (upper panel) and fresh-water flux (lower panel) through a cross-section near 80.5° N in Kennedy Channel. Data were collected over a short period in August 2003. Flow out of the Arctic has negative value. The horizontal line near the top of the lower frame marks the depth above which current was estimated, not measured

from one instrument at 100-m depth near Ellesmere Island has long been disquieting. Figure 9.14 shows the locations along the track of USCGC Healy where current profiles were measured during 7–11 August 2003; the coordinate axes associated with along and cross-channel flow are also shown. The observations were de-tided using tidal predictions (Padman and Erofeeva 2004), then averaged at each level within bins spanning 1 km across the channel and 50 km along it. Figure 9.15 is a cross-section of the along-channel current, which shows the dominant feature to be a southward subsurface jet peaking at 0.4 m/s only 2 km from Ellesmere Island. The depth of maximum speed was 150 m where the jet was 10-km wide. Current through the eastern part of the section was weaker, 0.05 m/s, and northwards. The calculated flux of volume through this section was also about 0.7 Sv in early August 2003, with the principal part within baroclinic subsurface jet on the Ellesmere side.

Prior to and during the survey in 2003, winds were persistent from the south-west (towards the Arctic), promoting down-welling on the Greenland side. Because the subsurface jet below 50-m depth ran counter to the wind, atmospheric conditions may have weakened the down-channel flow from values prevalent under more typical north-east wind. Three-year time series from Doppler sonar recently recovered from Nares Strait reveal a strong modulation of current at periods typical of synoptic meteorological forcing (Fig. 9.16). How the data from the surveys of August 2003 fit into this strong pattern of variability has yet to be determined. Nonetheless, the volume flux through Nares Strait at this time was comparable to the long-term average inflow through Bering Strait (0.8 Sv); the fresh-water flux was about half the estimated Bering Strait inflow (Woodgate and Aagaard 2005).
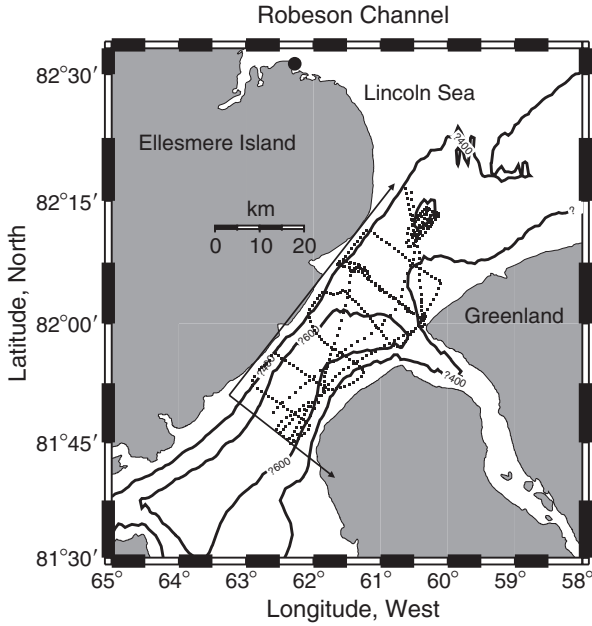
Fig. 9.14 Locations along the track of USCGC Healy where current profiles were measured during 7–11 August 2003
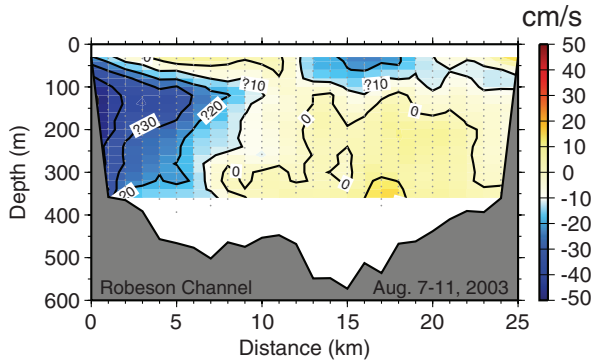
Fig. 9.15 Non-tidal current through Robeson Channel, 7–11 August 2003. Flow out of the Arctic has negative value. Note the wall-bounded southward jet on the Canadian side. The blank area near the top of the frame is too shallow for measurement by the hull-mounted sonar; that below 350 m is beyond the effective operating range of the sonar

The close correspondence in value between our volume flux and that of Sadler (1976) is fortuitous. However, the detailed picture from the 2003 survey does indicate that the dominant flux contribution in 1971 was from an instrument optimally positioned to measure the core of the sub-surface jet. We conclude that the suspicion attached
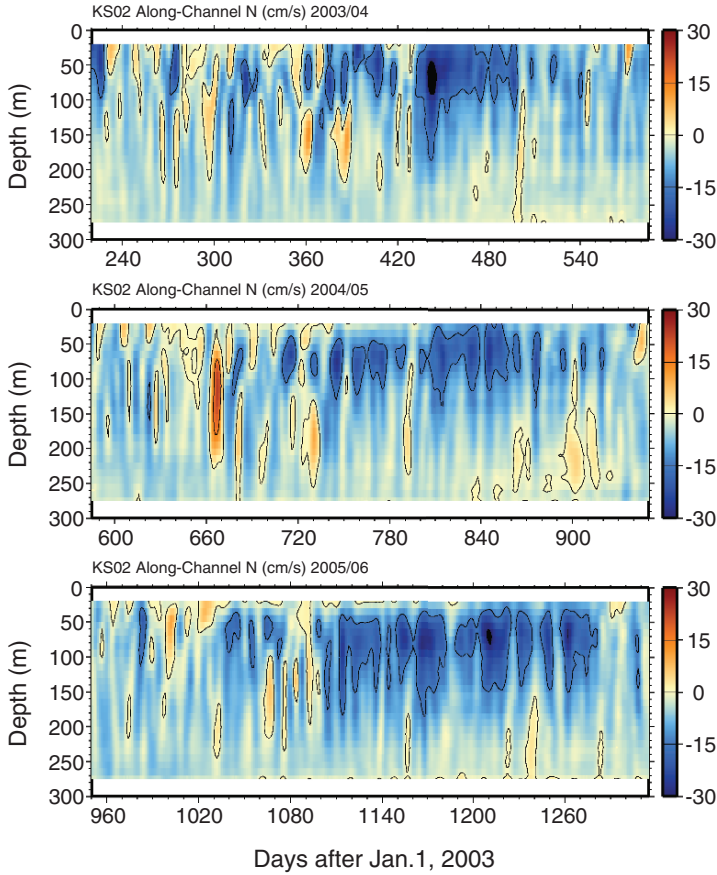
Fig. 9.16 Three-year time series of current along Kennedy Channel near Ellesmere Island from August 2003–2006; tides have been removed. Strong variability at periods typical of synoptic weather is obvious

to the uncharacteristically strong current measured by Sadler's instrument at 100-m depth was probably unwarranted. By inference this jet is apparently a persistent feature of Nares Strait through-flow.

9.6 Insights from Simulation of Canadian Arctic Circulation

Numerical models of fresh-water and ice movement through the Canadian Archipelago face formidable challenges. Principal among these are: (1) the scarcity of data to represent the three-dimensional structure of temperature and salinity and its seasonal variation; (2) the difficulty of resolving necessary detail in the many small but important passages while maintaining a correct dynamical interaction

between the modelled domain and bordering seas; (3) the weakness of sea-ice models in representing ice drift through channels, including the appearance and break-up of fast-ice and its influence on oceanic through-flow; and (4) realistic wind forcing of oceanic circulation. Until these challenges are met, our preoccupation is the realistic simulation of present conditions. Predictions of flow under future changed climate are fraught with uncertainty.

Nonetheless, there has been notable progress in the numerical simulation of fresh-water and ice movements through the Canadian Archipelago in recent years. Model-based flux estimates for seawater volume and fresh water are converging and models of pack-ice dynamics in island-studded waters have improved.

Advances have emerged from modern coastal-ocean models that have been implemented at high spatial resolution within the Canadian Archipelago. One model, Fundy, is linear and harmonic and a second Quoddy is non-linear and prognostic. The models have been built around the finite element method to best represent the geographic complexity of the area. In the present (2006) implementation, the horizontal triangular mesh has 76,000 nodes and 44,000 elements and a resolution ranging from 1.1 km in narrow straits to 53 km in Baffin Bay (Fig. 9.17). The vertical coordinate is resolved via a hybrid mesh with fixed levels over the upper 150 m, where the vertical stratification is strongest, and terrain-following computational surfaces at greater depths. The gridded density field has been developed iteratively,
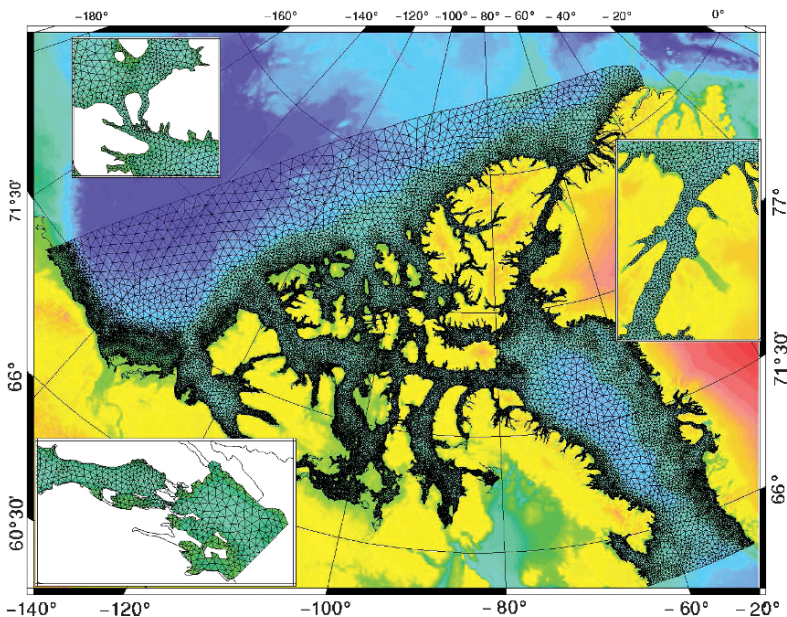

Fig. 9.17 The irregular triangular grid used for numerical simulation of circulation over the Canadian polar shelf. There are 76,000 elements (triangles) and 44,000 nodes (computation points). The mean separation of nodes is 7.8 km; the minimum and maximum are 1.1 and 80 km. Kliem and Greenberg (2003) used 20,000 elements and 12,000 nodes with 2.3–83 km separation

with the horizontal correlation scale inversely dependent on the density of hydrographic observations and directly proportional to the speed and orientation of calculated tidal flow. Fields of potential temperature and salinity for two seasons, summer and late winter, have been constructed from observational archives that span four decades. At present, sea ice appears only via a retarding effect on through-flow appropriate to the season; in other respects it is passive.

The tides are important to circulation within the Canadian Archipelago. They drive mixing and dissipation and control the boundary stresses (drag) in confined waterways. The properties of the tide vary with ice cover particularly near amphidromes where small changes in the amplitudes of incident and reflected waves can have a large impact on phase (Prinsenberg 1988; Prinsenberg and Bennett 1989). Dunphy et al. (2005) have computed a tidal mixing parameter based on modelled tides in the Archipelago. A map of this parameter reveals the regions of most intense tidal influence on mixing (Fig. 9.18), which match in some instances the locations of
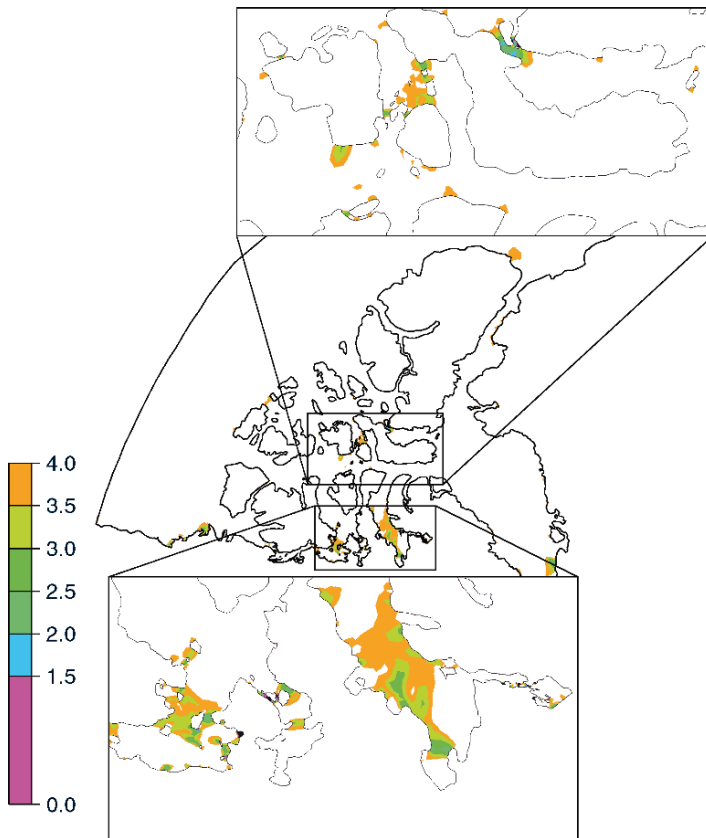
Fig. 9.18 The tidal mixing factor h/u^3 (contours are logarithmically spaced). Two regions with the smallest values (strongest mixing) are expanded for detail. The upper inset is centred on Hell Gate, Cardigan Strait, Queens Channel and Penny Strait. The lower is the region around the Boothia Peninsula (After Dunphy et al. 2005)

wintertime polynyas within the fast ice of the Archipelago. The dramatic inhomogeneity in tidal influence implies differences in water-mass evolution via mixing, heat loss and freeze-thaw cycling during through-flow depending on the path taken.

There are three runs involved in the simulation of the equilibrium through-flow. In the first, Fundy provides initial fields of sea-surface elevation and velocity from gridded fields of temperature and salinity. In the second, Quoddy is run diagnostically to incorporate tides and non-linear effects. The third run is prognostic. The simulations run for 10 days during each of the two observation-rich seasons, March–April and August–September. For sea-surface elevation along the inflow (viz. Arctic Ocean) boundary, average June–August values over 52 years have been used. These were computed using an updated version of the large-scale ocean model described by Holloway and Sou (2002). The value varies along the boundary and has an average value of about 0.1 m.

Not surprisingly, the diagnostic model reveals that the partition of through-flow among available pathways depends on the elevation difference between the Arctic Ocean and Baffin Bay and on baroclinic pressure gradients (viz. the distribution of temperature and salinity). For a representative 10-cm difference in sea level, the models yield a mean total through-flow of 0.9 Sv in summer (Kleim and Greenberg 2004). This value is smaller than numbers derived from observations (Melling 2000) but larger than the Steele et al. (1996) value derived from a simple ice–ocean model driven by observations of ice drift and concentration. Of the modelled total flux, 46% passes via Nares Strait, 20% via Cardigan Strait/Hell Gate and 34% via Lancaster Sound (Table 9.3). The model indicates that outflow via Lancaster Sound is supplied mostly from the Sverdrup Basin, with little contribution from Viscount Melville Sound and channels to the south (Fig. 9.19). This interesting outcome is consistent with observations reported by Fissel et al. (1988). The relationship between flux and sea-level difference is linear in the models (wherein hydrographic fields are fixed): a 5-cm increase in the sea level of the Arctic relative to Baffin Bay doubles the flux of volume.

The net volume flux reflects a balance between the barotropic pressure gradient, which drives water from the Arctic Ocean toward Baffin Bay, and the baroclinic pressure gradient which forces flow in the other direction. This is clear from Table 9.3 where the diagnostic result and that of a barotropic calculation using the same sea-surface elevation along the Arctic boundary are compared: the volume flux associated with barotropic forcing alone is five times larger. Clearly the baroclinic mode is an important aspect of circulation in the Canadian Archipelago. However, this result should not be viewed as an accurate measure of the relative contributions of the barotropic and baroclinic modes to flux. The ratio is suspect because it was derived using the diagnostic mode wherein the density field was specified (and of necessity grossly smoothed) and unresponsive to the circulation. Only a fully prognostic model can provide a realistic value for the ratio.

The diagnostic calculation has also provided values for the fresh-water flux. Values provided in Table 9.3 are subject to the cautions raised in the preceding paragraph. Typically, the model totals for all three routes of through-flow are approximately equal to values derived from observations in western Lancaster Sound alone (see Table 9.2), namely about 50 mSv (1,580 km^3/year) re 34.8.
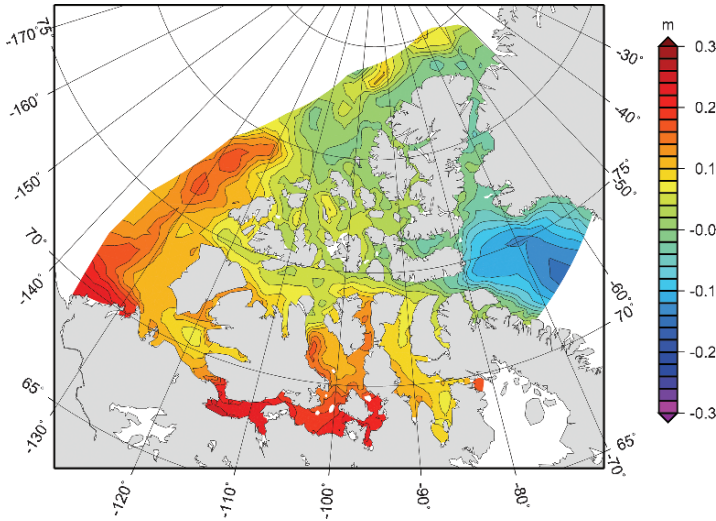
Fig. 9.19 Surface elevation as a proxy for transport, from a 3D non-linear diagnostic calculation. (Figure. 9.9 courtesy of Nicolai Kliem, DMI: http://ocean.dmi.dk/staff/nk/ArcticArchipelago/)

Table 9.3 Model-simulated fluxes of volume and fresh water through the Canadian Archipelago (after Kleim and Greenberg 2003). The reference salinity for fresh-water flux is 34.8. Arctic exports have positive value

| | Diagnostic | | Barotropic |
	Volume (Sv)	Fresh-water (mSv)	Volume (Sv)
Barrow Strait	0.3	20	1.8
Jones Sound	0.2	10	0.6
Nares Strait	0.4	20	2.4
Total	0.9	50	4.8

There have been few modelling studies with spatial mesh sufficiently fine to represent baroclinicity adequately within the narrow channels of the Canadian Archipelago. The coupled ice–ocean model of the US Navy Postgraduate School, which has 1/12th degree resolution (about 9 km), has been used for pan-Arctic simulations of the period 1979–2002 (Williams et al. 2004). The results indicate that the Canadian Arctic through-flow is the greater contributor (relative to Denmark Strait) of oceanic fresh water to the North Atlantic. According to the simulation, the fresh-water flux through the Archipelago has increased over the period studied, a trend that has perhaps contributed to decreasing salinity in the Labrador Sea.

The goal of future work is a prognostic model with time evolving fields of temperature and salinity. This is not a trivial undertaking, particularly on a terrain-following

mesh; methods with acceptable truncation error have been sought for many years. Such capability is essential for realistic simulation of baroclinic effects, including fresh-water and heat fluxes. An increase in resolution is also desirable, best accomplished for this area using the finite element method. The present best resolution is 1.1 km, barely adequate to represent important channels such a Hell Gate (4 km), Cardigan Strait (8 km) and Fury and Hecla Strait (1.8 km). Ocean circulation models need to be forced using wind fields that adequately reflect the important influence of topography and boundary-layer stratification on the mesoscale. Lastly, there is need for a realistic and fully interactive ice dynamics model; not only is pack ice an important element of ocean dynamics, but moving ice is itself a component of the fresh-water flux. The ice element may become a more important fraction fresh-water flux in a warmer climate, when ice of the Canadian Archipelago may be mobile longer each year (Melling 2002).

9.7   Ice Flux Across the Canadian Polar Shelf

Moving pack ice transports a fresh-water flux disproportionate to its thickness, by virtue of its low salinity (less than one tenth that of seawater) and of its position at the ice–atmosphere interface where it moves readily in response to wind. Both ice thickness and drift velocity are needed to calculate the sea-ice fresh-water flux. At present, ongoing observations of ice thickness are not available for any of the gateways discussed in this chapter. Here we concentrate on using satellite-based sensors to measure the movement of pack ice through the Canadian Archipelago. With supplementary guesses of pack-ice thickness, approximate values for the accompanying fresh-water flux can be provided.

The geography of the Canadian Archipelago is too complex for effective use of satellite-tracked drifters to measure the through-flow of pack ice. Methods based on the tracking of features in sequential images from satellite-borne sensors are better suited to the task. Microwave sensors provide the least interrupted time series of ice flux at key locations because they are relatively unaffected by cloud and wintertime darkness. However, the tracking of ice movement may be error-prone at times when ice features have poor contrast or when the pack is deforming appreciably as it moves; the latter is a common circumstance during rapid drift through narrow channels.

The displacement of sea ice over the interval between two images is derived by the method of maximum cross correlation (Agnew et al. 1997; Kwok et al. 1998). The technique works with sub-regions or patches on the two images that are 5–50 pixels on a side, depending on resolution. The underlying premise is that difference between consecutive images is the result of displacement only, the same for all features. Any additional rotation and straining of the ice field or creation of new ice features (e.g. leads) degrade the correlation.

Two long-term studies of ice movement through the Canadian Arctic have been completed. One used scenes acquired by synthetic-aperture radar at 0.2-km resolution (Radarsat: Kwok 2005; Kwok 2006) and the other utilized images

from a passive microwave scanner, which resolves ice features at approximately 6-km resolution (89 GHz AMSR-E: Agnew et al. 2006). Both approaches yield estimates of ice displacement and ice concentration at intervals of 1–3 days, constrained by the interval between repeated orbital sub-tracks.

The utility of AMSR-E is marginal in some parts of the Archipelago where channels are only a few pixels wide. Moreover, the 89-GHz channel is of little value during the thaw season (July–August) when the wet surface of the ice and high atmospheric moisture degrade image contrast; data acquired during the shoulder-months of June and September may also be poor at times. Microwave radar produces images of better contrast than microwave scanners during the thaw season, but the identification of floes and ice features from Radarsat can still be challenging during summer.

The flux estimates derived from microwave-emission images only incorporate ice motion that occurred during the cold months (October–May or September–June). Since this period overlaps significantly with fast-ice conditions within the Canadian Archipelago, the months of most active ice movement may have been missed. The flux estimates derived from Radarsat nominally span the entire year. However, it is noted that feature-tracking algorithms return a null result (low correlation) when the quality of images is poor or ice-field deformation is large; this fact may contribute a low bias to average displacement during the summer, when image contrast is poor and low ice concentration permits rapid movement and deformation of the pack.

Radarsat transmits microwaves and detects the energy back-scattered from the rough surface or upper few centimetres of the ice; it is not sensitive to ice thickness. AMSR-E detects natural microwave emission at several frequencies and polarizations, which can be manipulated to yield information on ice type and concentration. In general, satellite-based data on ice movement must be augmented by ice-thickness values from other sources if the flux of ice volume and fresh-water are to be estimated.

Kwok et al. (1999) calculated an area budget for Arctic multi-year ice during 1996–1997 using observations made from space by microwave scatterometer (NSCAT). They estimated an annual outflow from Nares Strait of 34×10^3 km^2 by mapping multi-year ice in northern Baffin Bay, presumed to have arrived here via Smith Sound. Subsequently, Kwok (2005) has used Radarsat images over a 6-year period (1996–2002) to measure directly the drift of ice through a 30-km wide gate at the northern end of Robeson Channel (Fig. 9.20). During these years, the average annual flux of ice from the Lincoln Sea into Nares Strait was 33×10^3 km^2, with an inter-annual span of ±50%. There was a strong annual cycle in ice drift, with the bulk of the transport during August through January; ice is typically fast in Nares Strait between mid winter and late July. The average volume flux of an assumed 4-m thickness of ice would have been 130 km^3/year (4 mSv).

For the years 1997–1998 to 2001–2002, Kwok (2006) has estimated ice-area transport across the main entrances to Canadian Archipelago from the west (Fig. 9.20): Amundsen Gulf, M'Clure Strait, Ballantyne Strait plus Wilkins Strait plus Prince Gustaf Sea (cf. Queen Elizabeth Islands south) and Peary Channel plus Sverdrup Channel (Queen Elizabeth Islands north). His results are summarized in Table 9.4. On average during the 5-year study, Amundsen Gulf was a source of ice for the
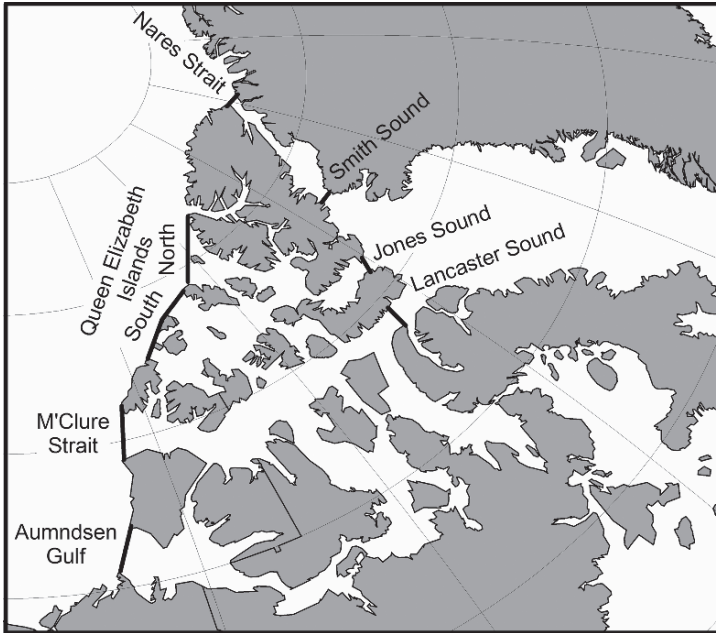
Fig. 9.20 Gateways within the Canadian Archipelago used in calculating the ice-area flux from sequential satellite images

Table 9.4 Annual average areal flux of ice between the Arctic Ocean and the Canadian polar shelf during the last decade. The unit is 1,000 km². Exports from the Arctic Ocean to the shelf have positive value

	Amundsen Gulf	M'Clure Strait	QEI south	QEI north	Nares Strait
1996–2002 (Sept.–Aug.)[a]	–	–	–	–	33 ± 13
1997–2002 (Sept.–Aug.)[b]	−85 ± 26	−20 ± 24	6 ± 5	2 ± 6	–
2002–2006 (Sept.–June)[c]	−14 ± 19	−5 ± 14	30 ± 8	6 ± 4	–

[a] Kwok (2005)

[b] Kwok et al. (2006)

[c] Agnew et al. (2006)

Arctic Ocean. Since the Gulf was ice-free during the summer, as typical, most of the export would be first-year ice leaving during autumn and winter. On assumption of 1-m average thickness (perhaps high because the gate traverses the Bathurst polynya), the average export would have been 85 km³/year. There was also an average export of ice from M'Clure Strait to the Beaufort Sea, although in smaller quantity and with occasional reversals (there was net import from the Beaufort in 2000). The average export would have been 80 km³/year, on assumption of 4-m average thickness

(McLaren et al. 1984). Only the entry points to the Sverdrup Basin accepted a net influx of ice to the Canadian polar shelf, but the amount was small (8×10^3 km²/year or 7 km³/year if ice was 3.4 m thick). This net influx is consistent with the analysis of Melling (2002), although its value is only about 20% of that implied by Melling's analysis.

The analysis has been extended to the cold months of 2002–2003 to 2005–2006 using AMSR-E (Agnew et al. 2006). The pattern of flux, with export from Amundsen Gulf and M'Clure Strait and import into the Sverdrup Basin, was continued during this period. However, the average out-fluxes from Amundsen Gulf and M'Clure Strait during this 4-year period (14 and 5×10^3 km²/year) were smaller than during the preceding 5-year period (85 and 20×10^3 km²/year) and the influxes to the Sverdrup Basin (30 and 6×10^3 km²/year) were larger (6 and 2×10^3 km²/year). There is obviously inter-decadal variability, as inferred by Melling (2002), which may respond to cycles in atmospheric circulation; it may also be that ingress of pack ice to the Sverdrup Basin was easier after the extensive loss of old ice within the Archipelago in 1998.

On the other side of the Canadian Archipelago, ice generally moves from the Canadian polar shelf into Baffin Bay. Agnew et al. (2006) have also used images acquired via AMSR-E to estimate ice flux into Baffin Bay during the colder months of 2002–2003 to 2005–2006: annual average fluxes were 48, 10 and 9×10^3 km²/year via Lancaster, Jones and Smith Sound, respectively. The associated fluxes of volume were 49, 10 and 9 km³/year per metre of ice thickness.

Agnew and Vandeweghe (2005) have calculated the ice flux during 2002–2004 through a gate across central Baffin Bay; the average over the 2-year interval was 690×10^3 km²/year southward. Clearly the efflux of ice from the Canadian polar shelf during the last decade has been larger than the influx, implying that much of the ice exported to the Labrador Sea has been formed there and not in the Arctic Ocean itself. Moreover, the southward flux of ice through Baffin Bay actually exceeded that through Fram Strait over the same period in terms of area (590×10^3 km²/year: Agnew and Vandeweghe 2005). However because the Fram Strait flux is primarily old ice and that the Baffin flux is primarily seasonal, the export of ice volume through Baffin Bay is probably the lesser.

Table 9.5 summarizes the ice flux values discussed here.

Table 9.5 Annual average areal flux of ice between the Canadian polar shelf and Baffin Bay during the last decade. The unit is 1,000 km². Arctic exports have positive value

	Lancaster Sound	Jones Sound	Smith Sound	Baffin Bay	Davis Strait
1996–2002 (Oct.–Apr.)[a]	–	–	34 ± 9	–	–
2002–2004 (Oct.–May)[b]	–	–	–	690 ± 80	610 ± 70
2002–2006 (Sept.–June)[c]	48 ± 6	10 ± 3	9 ± 2	–	–

[a] Kwok et al. (1999)

[b] Agnew and Vandeweghe (2005)

[c] Agnew et al. (2006)

9.8   Terrain-Channelled Wind and Oceanic Fluxes

The probable prime mover of the Pacific-Arctic through-flow is a decrease in sea level between the Pacific and the Atlantic. However, evidence for supplementary forcing of flows via internal gradients of pressure in the ocean and by winds has already been discussed. A strong channelling of airflow through Arctic straits, with consequent amplification of wind forcing on the ocean is a recent discovery. Its effect is discussed here in relation to Nares Strait, where it is possibly most influential. However, it is likely a factor at all gateways of interest to the Arctic fresh-water budget.

The flow of seawater through the Canadian Archipelago is variable but persistent. However, the flow of ice through the narrow waterways is strongly constrained by material stresses within the pack. In most channels, high ice concentration and low ice temperature during the cold season are sufficient to halt ice drift. One consequence is the cessation of fresh-water flux via moving ice. A second is the isolation of oceanic flows from stresses exerted by wind. A third is increased drag on the flow of water imposed by friction at the ice-water interface.

Pack ice in Nares Strait usually consolidates in winter behind an ice bridge at its southern end in Smith Sound (Agnew 1998). Consolidation can occur any time between November and April, and may occur in stages, with bridges forming consecutively in Robeson Channel (northern end), Kennedy Channel (middle section) and Smith Sound, perhaps to collapse a few weeks later or perhaps to remain as late as August. Such variability suggests that the fast-ice regime of Nares Strait is of marginal stability in the present climate, flitting between the permanent mobility typical of Fram Strait and the reliably static winter ice of the western Archipelago.

It is plausible that topographically amplified winds in Nares Strait contribute to the intermittent instability of fast ice in the channel. However because there are no systematic long-term observations of wind in the area, present insights have been derived via numerical simulation (Samelson et al. 2006) using the Polar MM5 mesoscale atmospheric model (Bromwich et al. 2001). This is a version of the Pennsylvania State/NCAR MM5 (non-hydrostatic, primitive-equation, terrain-following, full moist physics) which has been optimized for the polar environment (Cassano et al. 2001; Guo et al. 2003). The configuration is triply nested, from 54- to 18-km to 6-km grids. It has been run daily at Oregon State University since August 2003 in a 36-h forecast mode, with initial and time-dependent boundary conditions taken from the operational AVN model of the US National Center for Environmental Prediction.

Strong radiational cooling at the surface in polar regions commonly creates a stable planetary boundary layer in winter (Bradley et al. 1992; Kahl et al. 1992), wherein wind may be strongly channelled through areas of low terrain. The mesoscale model commonly generates an intense boundary-layer jet at elevation below that of the confining terrain. Moreover, the along-channel wind speed is well correlated with the difference in sea-level pressure along Nares Strait (Samelson et al. 2006). The along-channel balance indicates that the atmospheric jet is an ageostrophic response to orography. The drop in sea-level pressure along the 550-km long strait can exceed 25 mb, with simulated winds reaching 40 m/s at 300-m elevation.

Mesoscale processes are clearly influential in accelerating airflow through Nares Strait: high terrain on both sides, the unusual length of the channel and its narrow width isolate air flow from the synoptic-scale geostrophic constraint; the strong ageostrophic response to pressure gradient is only weakly damped by momentum transfer through the stable boundary layer and is locally amplified by effects of varying channel width. Moreover regional synoptic climatology is a contributing factor because Nares Strait is a short-cut between two different synoptic regimes, the Polar high and the Icelandic low. Figure 9.21, depicting the regional variation in sea-level pressure from the MM5, clearly reveals both synoptic-scale and mesoscale factors: the large difference in pressure between the Lincoln Sea and Baffin Bay and the two zones of steep pressure gradient and strong along-channel wind, in Kennedy Channel and in northern Baffin Bay. The probable along-channel force balance involves the pressure gradient, inertia and friction while the cross-channel balance is geostrophic (on the mesoscale). Boundary stress likely fades to insignificance above a few hundred meters, leaving an inviscid balance in the upper part of the jet.

The dynamical explanation for the wind maxima at two locations, where Kennedy Channel widens into Kane Basin and again where Smith Sound widens into Baffin Bay may be super-critical flow. This phenomenon is known to create similar expansion fans in summer in the lee of capes on the US west coast (Winant et al. 1988; Samelson and Lentz 1994). Pressure gradients develop as the inversion-capped
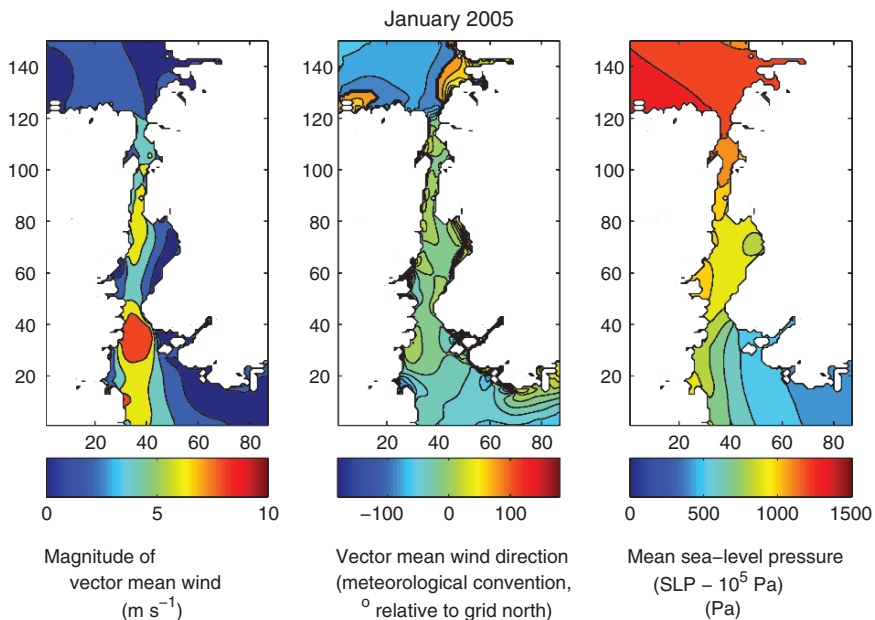

Fig. 9.21 Average fields of vector wind and sea-level pressure for January 2005. These data from simulations using the MM5 clearly reveal meteorological features on both synoptic and meso scales

marine boundary layer thins where the channel widens; these gradients in turn force ageostrophic acceleration.

Empirical orthogonal functions computed from monthly averages of simulated airflow and surface stress over a 2-year period (Fig. 9.22) show that the time-dependent flow has a spatial structure very similar to that of the mean flow, shown for January 2005 in Fig. 9.21. The annual cycle was energetic during this particular period: the average airflow alternated between strongly southward during October through January and northward in July and August.

Variance in the synoptic band of frequency was suppressed by the monthly averaging applied in the preparation of Fig. 9.22. Nonetheless, this band is very energetic in Nares Strait. Figure 9.23 displays the along-channel surface wind for a 1-year period. Values have been derived from the along-channel difference in sea-level pressure (Carey Islands minus Alert) using the regression line calculated by Samelson et al. (2006), but comparable fluctuations are apparent in simulated winds.

Simulations of mesoscale atmospheric flow within the Canadian Archipelago have been focussed to date on Nares Strait. However, it is likely that each of the six constrictions to through-flow in the oceanic domain – Nares Strait, Hell Gate, Cardigan Strait, Lancaster Sound, Bering Strait and Davis Strait – have some impact on the speed and direction of winds. The intensity of mesoscale influence likely differs within the group, since the straits encompass a wide range of dimensions in terms of height of terrain (200–2,000 m), width of strait (8–350 km), length of strait
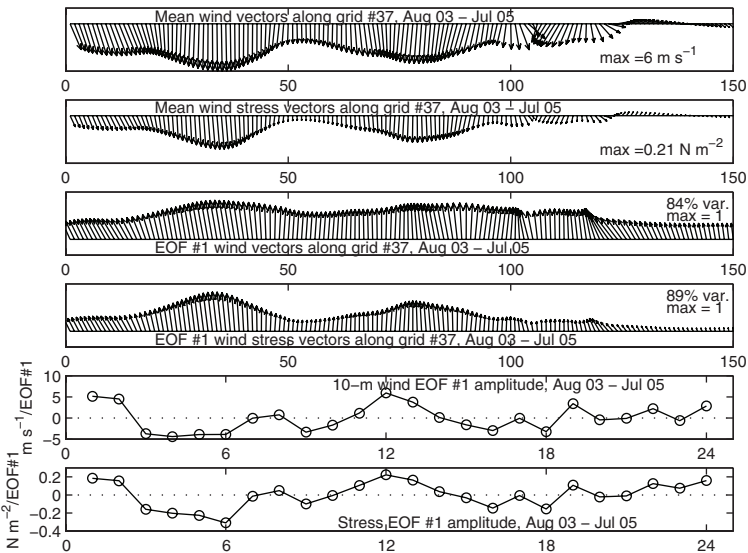
Fig. 9.22 The top four panels display the mean wind, the mean wind stress and their primary empirical orthogonal functions. The horizontal coordinate (grid node) increases along a line running up Nares Strait from Baffin Bay to the Lincoln Sea; node 50 and 80 are in Smith sound and southern Kennedy Channel, respectively. The bottom two panels display the eigenvalues plotted against month, for 2 years beginning in August 2003
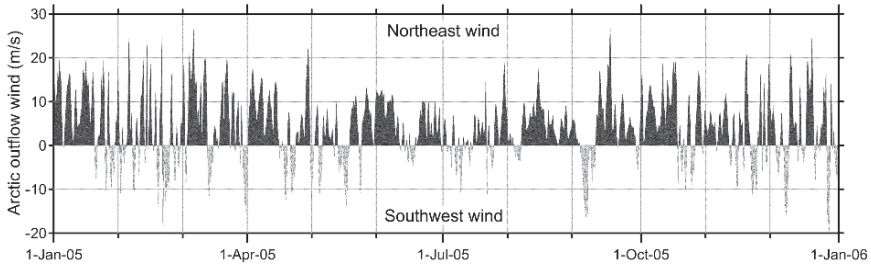
Fig. 9.23 Year-long series of along-channel surface wind in Nares Strait, calculated using the linear dependence of wind on the along-channel difference in sea-level pressure established by Samelson et al. (2006). Pressure was measured at Alert and on the Carey Islands

(0–550 km) and latitude. The latter may influence boundary-layer stability through its direct and indirect effects on insolation, surface albedo and surface emissivity. Based on our presently incomplete understanding of these effects within Nares Strait, we rank the straits in the following sequence of decreasing sensitivity to wind amplification on the mesoscale: Nares Strait, Cardigan Strait/Hell Gate, Lancaster Sound, Davis Strait, Bering Strait.

9.9 Geochemical Identification of Sources for Canadian Arctic Outflow

Knowledge of the magnitude and causes of fresh-water flux through the North American Arctic is the primary objective of the present study. However, knowledge of the sources of the fresh water is essential to understanding the roles of the fresh-water flux in the global hydrologic cycle and climate system. The trace geochemical signatures of seawater can provide clues about the sources, transit times and history of the through-flow.

Although the primary indicator of fresh water in the ocean is salinity, a number of trace chemical constituents can provide insight into fresh-water origin and transport within the Arctic. Recent studies that illustrate the application of chemical tracers to Arctic fresh-water issues have been published by Cooper et al. (1997), Jones et al. (1998), Smith et al. (1999), Schlosser et al. (2000), Ekwurzel et al. (2001), Amon et al. (2003), Jones et al. (2003), Taylor et al. (2003), Alkire et al. (2006), Falkner et al. (2006), Yamamoto-Kawai et al. (2005), Yamamoto-Kawai et al. (2006) and Jones and Anderson (2007). Exploited dissolved trace chemicals include nutrients, molecular oxygen, alkalinity, chlorofluorocarbons, natural and artificial radionuclides, barium and other trace metals, organic matter and heavy isotopes ^{18}O and ^{2}H in water molecules.

The interpretation of the first exploratory sampling of tracers in Arctic waters was constrained by poor geographic coverage. Data from several expeditions, perhaps

spanning several years, were typically aggregated or averaged to draw maps of tracer distributions. Interpretation was necessarily based on the assumption of steady ocean circulation. Increased effort in data collection over the last decade has permitted a more rewarding focus on temporal variability. Here we discuss new knowledge emerging from tracer hydrography in the western hemisphere of the Arctic, with particular attention to temporal variability in the relative contributions from various sources of fresh water. In future years, a significantly improved understanding should emerge from the time series of strictly comparable data that are now being produced.

The interpretation of oceanographic tracers in the North American Arctic presents special challenges. For example, the wide range in surface conditions from year-round ice to seasonal ice zones, from fast ice to ice-free seas may render inappropriate simple assumptions applied elsewhere regarding the impacts of biology and ventilation on tracer concentrations. Interpretation of tracer distribution can be ambiguous. Baffin Bay for example receives Arctic waters via two paths, from the north via the Canadian Archipelago and from the south via the West Greenland Current. Moreover, fresh water with large and variable $\delta^{18}O$ anomalies from melting ice sheets in Greenland and northern Canada (which also contribute glacial flour) increases the complexity of geochemical interpretation.

Dissolved nutrients and oxygen have the longest history among all chemical tracers used in ocean science, in the Arctic as in temperate waters. A relatively high concentration of silicic acid ($[Si] \geq 15\,mmol\,m^{-3}$) has long been known to distinguish waters that enter the Arctic from the Pacific via Bering Strait; this influx can be traced as a relative maximum in dissolved silica concentration (coincident with a maximum in dissolved phosphorus $[P]$ and coupled with a minimum in dissolved oxygen $[O_2]$) in the halocline (Kinney et al. 1970; Codispoti and Lowman 1973; Jones and Anderson 1990). Recent interpretation that additionally utilizes $\delta^{18}O$ has revealed that the dissolved nutrient and oxygen in the Arctic halocline result primarily from the Bering Strait inflow in winter (Cooper et al. 1997, 2006). In the sunlit half of the year, biological cycles of growth and decay change the concentrations of dissolved nutrients and oxygen. Biological impact on the Pacific inflow is further amplified in summer when the inflow is less saline (therefore closer to the surface) and free of light-obstructing ice cover. Tracing the movement of Bering Sea water that enters the Arctic during spring, summer and autumn demands ingenuity in geochemical interpretation.

Within the Canadian Archipelago, the earliest reliable cross-sections of dissolved silica were observed in the summer of 1977. The concentration was highest in Lancaster Sound, intermediate in Jones Sound and lowest in Smith Sound. This gradation was taken to indicate that water (and fresh water) from the Pacific was unlikely to reach the Lincoln Sea and contribute to the flow through Nares Strait (Jones and Coote 1980).

This conclusion was revised when the co-variation of dissolved nitrate and phosphate was developed as a discriminant of Pacific from Atlantic-derived waters within the Arctic (Jones et al. 1998; Alkire et al. 2006; Yamamoto-Kawai et al. 2006). De-nitrification of inflowing seawater occurs over the shallow shelves of the

Chukchi and northern Bering Seas. This process renders the Pacific inflow deficient in fixed inorganic nitrogen relative to Atlantic water. Within the Arctic Ocean, biological action tends to move the nitrate and phosphate concentrations within each contributing water mass (Pacific and Atlantic) along lines of constant "Redfield-like" slope on a nitrate-versus-phosphate diagram. Because mixtures of Pacific and Atlantic waters have concentrations of these two constituents that fall between the source-water reference lines; the position between the reference lines on the diagram indicates the fractions of Pacific and Atlantic water in the mixture.

Complications arise with the contribution of water from other sources, such as rivers and melting ice. To a first approximation, however, studies of $\delta^{18}O$ reveal that these interfering contributions are generally less than 10% within the Arctic Ocean (Östlund and Hut 1984) and that rivers provide nutrients in proportions resembling those characteristic of Atlantic water (Jones et al. 1998). The nitrate–phosphate (N–P) method for discriminating Pacific from Atlantic waters has recently been refined to include the contribution of ammonium and nitrite to the fixed inorganic nitrogen. The quality of the analysis has improved because ammonium is an appreciably component of the nitrogen dissolved in Pacific-derived seawater (Yamamoto-Kawai et al. 2006).

Jones et al. (2003) have applied the N-P method to track the Pacific influence in Arctic through-flow within the Canadian Arctic and the Labrador Sea and through Fram Strait to Denmark Strait. From sections measured in August 1997, they concluded that Pacific inflow completely dominated the seawater end member in Barrow Strait and provided at least three quarters of this end member in the topmost 100 m of Jones and Smith Sounds; Pacific water was similarly prevalent that year within 100 km of Baffin Island in Davis Strait. It was detected in diluted (50%) form with somewhat variable extent over the Labrador shelf in 1993, 1995 and 1998 and as far south as the Grand Banks in 1995.

The magnitude of Pacific influence in waters south of Davis Strait may be an over-estimate because de-nitrification likely occurs also in the relatively shallow waters of Hudson Bay. N*[1] is a nutrient-based parameter that has negative value in de-nitrified water. In the North Atlantic, values of N* are near zero or positive. Values of N* are negative for Pacific waters passing through Bering Strait and about $-12\,\mu M/kg$ for water in Barrow Strait (Falkner et al. 2006). Unpublished data from Hudson Bay in the summer of 1982 (Bedford Institute of Oceanography, DFO Canada) reveal water with N* even more negative (-23 to $-12\,\mu M/kg$). Because the deepest waters of Hudson Bay (S ~ 33.5) are replaced on a time scale of about a decade (Roff and Legendre 1986), Atlantic water supplied to Hudson Bay via Hudson Strait could be de-nitrified to a Pacific-like signature before re-emergence into the Labrador Sea. Such occurrence would complicate the N–P interpretation wherever there is influence from Hudson Bay.

---

[1] N* ($\mu M/kg$) = $[NO_3]$ – $16\cdot[PO_4]$ + 2.90. N* was first defined by Gruber and Sarmiento (1997) and modified by Deutsch et al. (2001).

A recent analysis that combines measurements of tracer concentration and current velocity on several sections across Nares Strait is a valuable innovation (Falkner et al. 2006). Current measurements by ship-mounted ADCP in August 2003 delineated a southward flowing jet at 100–200 m depth along the western side of Nares Strait; simultaneous hydrographic sections revealed an enrichment of silica and phosphorus in this jet that was indicative of origin as wintertime Arctic inflow through Bering Strait. N–P analysis has shown that the only seawater end-member in the upper 100 m at the northern end of Nares Strait was Pacific water, but that Pacific water shared equal status with Atlantic water in the marine component at the southern end (Smith Sound). Clearly, there had been appreciable mixing between the south-flowing Pacific water and north-flowing Atlantic water (from the West Greenland Current) during transit. Pacific influence in the mixture at this section in 2003 was appreciably more dilute than in 1987. Subsequent comparison of nutrient measurements in August of various years has revealed inter-annual variability (Fig. 9.24), comparable for silica to that proposed as seasonal in the interpretation of a 10-month series from the North Water in 1997–1998 (Tremblay et al. 2002).

Figure 9.24 displays nutrient concentration for various years in Canadian Arctic straits with inflows from both the Arctic Ocean and Baffin Bay. The
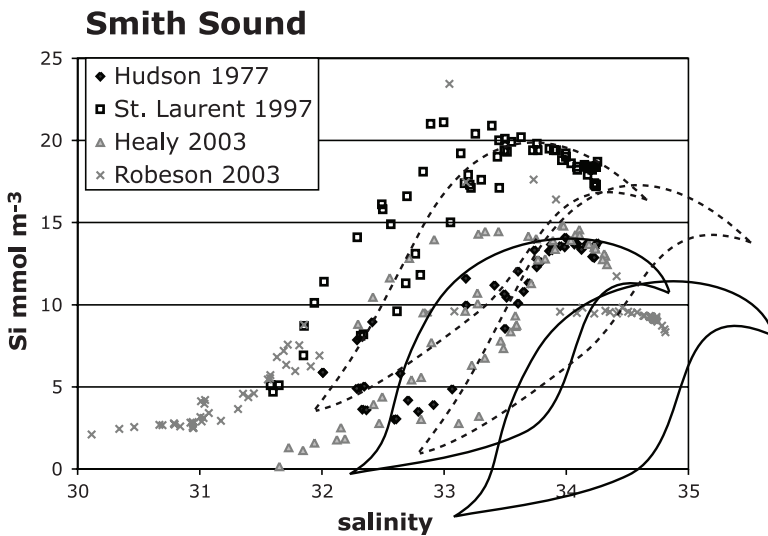
Fig. 9.24 Silicate versus salinity for seawater samples acquired in Smith Sound during August of several years. Added curves envelope data from 1977 and 2003 (solid lines) and from 1997 (dashed line). Within both envelopes, the concentration is highest on the western side of the straits. Note the high silica concentration (strong Pacific influence) in Robeson Channel in 2003, values comparable to those measured 600 km to the south in Smith Sound in 1997 (Falkner et al. 2006)

envelopes that enclose these data are shifted toward higher nutrient concentration (viz. greater Arctic influence) in August 1997 than in 1977 and 2003 (Falkner et al. 2006). The simplest interpretation is that the flux of nutrient rich Pacific water (plus meteoric and ice-melt waters mixed with it) was higher in all the straits in August 1997 than in 1977 and 2003. The higher flux occurred just after the prolonged positive anomaly in the Arctic Oscillation Index (AO) during 1989–1995.

What is the mechanism via which the AO, which is an expression atmospheric pressure distribution over the northern hemisphere in winter, might influence oceanic circulation and fluxes in summer? Proshutinsky and Johnson (1997) have used a barotropic ocean model to demonstrate that the Arctic Ocean responds to the AO in a basin-wide oscillation with cyclonic and anti-cyclonic anomalies: higher peripheral sea level results from the set-up of low salinity water against the ocean boundary under high AO forcing. A subsequent study based on a more realistic ice-ocean model was forced by NCEP-reanalysis winds for 1951–2002 (Häkkinen and Proshutinsky 2004). Various measures of the Arctic Ocean Oscillation, including sea surface height, all co-varied with the Arctic (Atmosphere) Oscillation. During the years of unusually high AO, 1989–1996, the model indicated a sustained loss of fresh water from the Arctic Ocean, which had by 1997 created the most negative fresh-water anomaly of the entire 50-year simulation. Although Häkkinen and Proshutinsky (2004) do not comment on whether the exported fresh water passed to the east or to the west of Greenland, the timing meshes with the inference of Falkner et al. (2006) based on geochemical analysis of Canadian Arctic through-flow in 1997. Interestingly, the inflow of Atlantic water was an essential element in the wind-driven barotropic response to the AO; it was the factor most strongly correlated with fresh-water anomalies within the basin.

Additional trace compounds can be used to distinguish the meteoric (river inflow plus precipitation) and ice-melt components of Canadian Arctic through-flow. For example, Jones and Anderson (this volume) discuss the use of seawater alkalinity for this purpose. Östlund and Hut (1984) pioneered the mass-balance analysis of the seawater isotopic composition in the Arctic to distinguish run-off from ice melt-water as freshening agents. Within the Canadian Archipelago and east of Greenland, a more complicated analysis may be required. As discussed by Strain and Tan (1993), the separation of salt and water by the freeze-thaw process can, in combination with mixing under conditions prevalent in Baffin Bay, generate a seasonal cycle in the $\delta^{18}O$ value for the zero-salinity end-member. The $\delta^{18}O$ values can vary from that typical of summertime precipitation ($\delta^{18}O \approx -10$) to that typical of glacial melt-water ($\delta^{18}O \leq \approx 25$). In the big picture, direct contributions of fresh-water via precipitation and ablation of ice sheets are small relative to those via Arctic rivers ($\delta^{18}O \approx -20$) and Pacific inflow ($\delta^{18}O \approx -1$). However, they may be important in the principal Arctic fresh-water outflows because of proximity to the ice sheets of Greenland and of the Canadian Arctic Cordillera. An ideal analysis would be expanded to incorporate additional tracers and contextual information so that artefacts can be identified.

9.10   Gateway to the Atlantic, Davis Strait

All streams of Arctic water that cross the Canadian polar shelf enter Baffin Bay, with the exception of about 0.1 Sv that is diverted along the western side of Baffin Island via Fury and Hecla Strait (Barber 1965; Sadler 1982). These streams join the cyclonic circulation of the West Greenland Current (itself fed by Arctic outflow via Fram Strait) to form the Baffin Current, which follows the continental slope of Baffin Island and enters the Labrador Sea through Davis Strait.

The properties of Arctic seawater and ice are modified by freezing, thawing, terrestrial and glacial run-off and mixing during their transit across the Canadian polar shelf (more than 1 million square kilometers of ocean area) and through Baffin Bay (an additional 2/3 million square kilometers) to Davis Strait. Although the residence times for through-flowing water and ice are not known, they are likely significantly longer than the most rapid transit (by ice from the Lincoln Sea to Davis Strait), which requires about a year. Ultimately, it is this modified Arctic water mass that affects deep water formation in the Labrador Sea. Davis Strait is a suitable location to measure the sum of all Arctic outflows via routes west of Greenland at a single section just prior to their entry into the convective gyres of the north-west Atlantic.

The operation of a moored array to measure volume and fresh-water fluxes through Davis Strait is not a trivial undertaking. The narrowest part of the strait is 330 km, with 200 km of this span deeper than 500 m; the maximum depth is close to 1,000 m at the narrowest point, but shoals to 700 m at the sill. There is a topographic spur that extends along the axis of the Strait and likely influences flow near the sill. Relative to the internal Rossby scale (here about 25 km), the Strait is dynamically wide, admitting small eddies and recirculation that must be resolved to obtain accurate estimates of fluxes. The upper few hundred metres, particularly on the Canadian side, are swept by a broad stream of icebergs moving south with the current; this is a big risk to instrumented sub-sea moorings within the Arctic outflow. There is a strong counter-flow (the West Greenland Current) on the eastern side of the Strait, with a front, eddies and re-circulation features in the region where the two currents interact over the broad flat sill.

The water masses and circulation within Davis Strait during the ice-free season have been mapped using hydrographic surveys and satellite-based temperature scanners. The 500-m isobath on Fig. 9.25 reveals the broad extent of the continental shelf (150 km on the Greenland side) and the coloured underlay depicts the mean sea-surface temperature in September. Water warmer than 4 °C (fresher than 33) in the Labrador Sea and over the Greenland shelf is carried northward by the West Greenland Current; it is a mixture of Atlantic water and outflow from Fram Strait. Most of this stream turns west and then south following isobaths into the northern Labrador Sea; some continues northward along the Greenland shelf. Vectors in Fig. 9.25 represent depth-averages of measured current; they confirm the inference from sea-surface temperature of a northward flow on the Greenland side and a southward flow of Arctic water on the Canadian side.
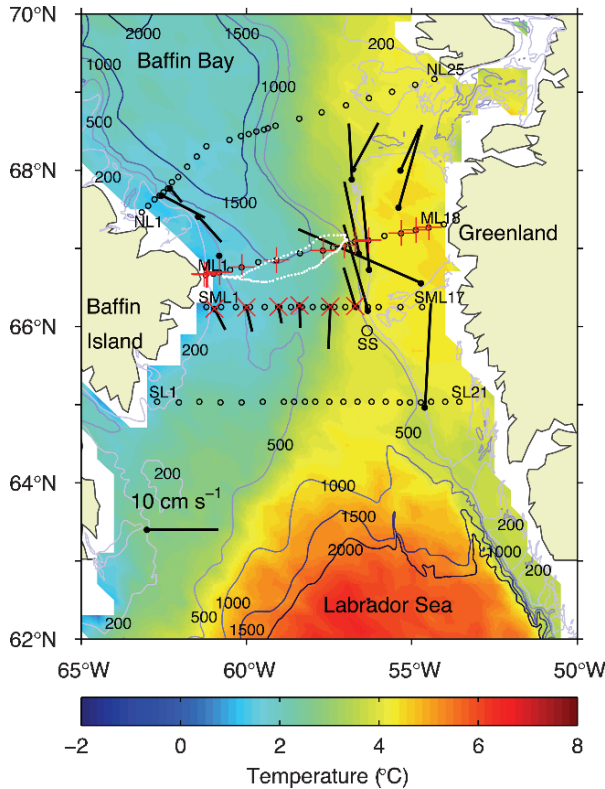
Fig. 9.25 Bathymetry of Davis Strait. The coloured underlay represents long-term mean sea-surface temperature. Red 'x' mark the positions of the 1987–1990 moorings (Ross 1992); Red '+' mark the locations of moorings placed in September 2004 in the new initiative to measure oceanic fluxes. Open circles mark recent hydrographic surveys. The white dotted line is the 2006 Seaglider track. Vectors depict depth-averaged current from instruments on moorings in the 1980s

There are three principal water masses in Davis Strait (Tang et al. 2004): Arctic Water, West Greenland Intermediate Water originating in the Atlantic and Baffin Bay Deep Water (below 800 m). Figure 9.26 displays their distribution across a hydrographic section measured at 25-km resolution in September 2004. Here West Greenland Intermediate Water is warmer than 2 °C, more saline than 34.5 and extends from the Greenland slope into mid-strait below 50-m depth; a smaller core of this water over the Baffin slope is likely a recently separated filament that is returning southward. Arctic water colder than 0 °C and fresher than 33.5 fills the upper 250 m of the western half of Davis Strait; here the salinity anomaly (referenced to 34.8) is quite large in a thin layer within 50 m of the surface. Both this thin layer and the sharp front that separates Arctic from Atlantic-derived water present significant challenges to the measurement of the flow and salinity structure needed to calculate fresh-water flux.
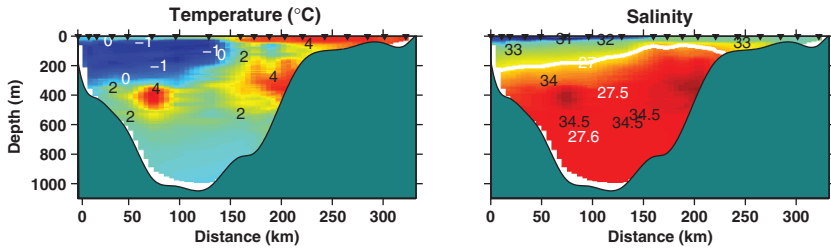
Fig. 9.26 Hydrographic section across Davis Strait (ML line) measured in September 2004, showing temperature (°C, left panel) and salinity (right panel). The station spacing was about 25 km
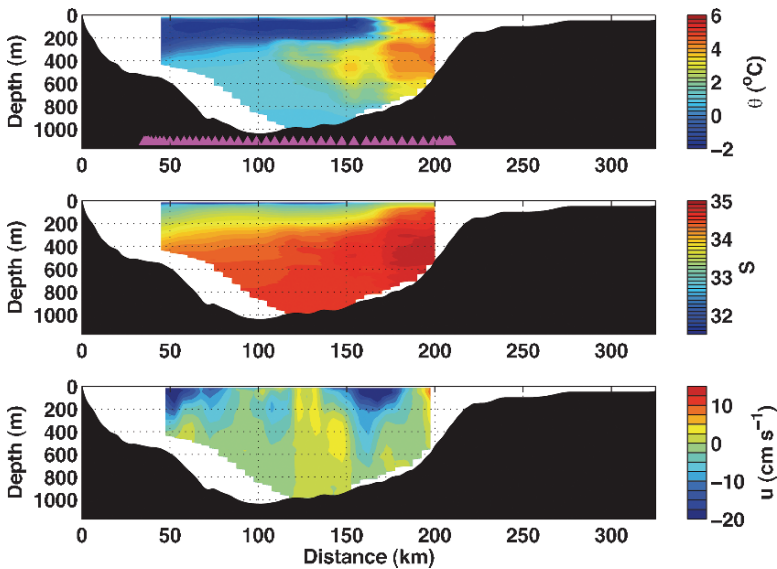
Fig. 9.27 Hydrographic structure within the deep trough of Davis Strait measured by Sea Glider at approximately 5-km resolution in September 2006

Hydrographic sections measured recently at much higher resolution (5 km) by Seaglider (see Chapter 25) illustrate the challenge posed by meso-scale structure within Davis Strait (Fig. 9.27). Even at this fine station spacing, there is plentiful detail in temperature, salinity and geostrophic shear at the limit of resolution; average values of current for the upper 1,000 m (estimated from glider navigation) uncover analogous variation in flow. The high-resolution section also reveals the large fresh-water anomaly of the thin surface layer. The rapid movement of this surface layer represents a substantial fraction of the fresh-water flux in Arctic waters (Melling 2000). For example, use of the salinity at 100-m depth (the shallowest measurement from the present array) to represent the salinity above this

level over a 150-km span with a 0.1 m/s current results in an under-estimate of fresh-water flux by 23–32 mSv, depending on the month.

During 1987–1990, Fisheries and Oceans Canada maintained an array of conventional current meters (current, temperature, salinity at 150, 300 and 500 m) on five moorings along the 66.25° N (Ross 1992). The array spanned the deep central trough at roughly 50-km spacing. Because instruments were not placed shallower than 150 m, where iceberg risk is high, the array did not cross the shelves or sample the low-salinity Arctic outflow. In addition, Tang et al. (2004) and Cuny et al. (2005) report low correlations between time series from instruments on different moorings, indicating that the array failed to resolve flows at the scale of variability within the Strait. Because of these shortcomings, the data were ill-suited to flux estimation. Nonetheless, Cuny et al. (2005) calculated fluxes on assumption that: (1) temperature and the salinity were constant above 150 m when the sea was ice-covered; (2) seasonally appropriate recent or archived data provided valid vertical gradients above 150 m during ice-free months; (3) upper ocean profiles could be estimated by shifting climatological data to match daily values observed at 150 m; (4) measured daily current speed at 150 m provided known motion at a reference level for calculated geostrophic current; and (5) values varied linearly between moorings. Fluxes over adjacent continental shelves were ignored. Tang et al. (2004) have used the same data under slightly different assumptions; principally they substituted climatological values for salinity gradient in the upper ocean year-round.

The upper part of Table 9.6 summarizes volume and fresh-water flux estimates out of the Arctic derived from these older data. Values based on the long-term, but under-resolved, direct observations average about 3.1 Sv and 125 mSv (3,940 km³/year), respectively (Loder et al. 1998; Tang et al. 2004; Cuny et al. 2005). Fluxes passing along the Greenland shelf have not been included; Cuny et al. (2005) estimate these as −0.8 Sv and −38 mSv (1,200 km³/year), so that their corrected net fluxes for the entire Strait are 2.3 Sv and 87 mSv (2,750 km³/year). The hydrographic surveys in September provide better horizontal resolution and include the shelves but because they are snapshots, the derived flux estimates are more variable year to year, ranging over 1.5–5.7 Sv and 126–286 mSv (3,980–9,020 km³/year). It is plausible (and consistent with some observations within the Archipelago) that the fluxes might actually be larger in September than in annual average.

The lower part of Table 9.6 summarizes preliminary flux estimates derived from the ongoing USA–Canada Fresh-water Initiative that is acquiring data from a new and larger moored array and from hydrographic surveys by ship and Seaglider. The present summary is preliminary, derived from an independent consideration of each source of data. Geostrophic calculations referenced to zero at the seabed and averaged over four sections yield volume fluxes of 1.8 ± 1.5 Sv and 2.3 ± 0.9 Sv for September 2004 and 2005. A simplistic estimate based on data from moored instruments during 2004–2005 (including some measurements over the shelves) is an annual mean value of 2 Sv, with large uncertainty. Preliminary estimates of fresh-water flux from the ship CTD survey in September 2004 and the September/October 2005 transects by

Table 9.6 Estimates of the net fluxes of volume and fresh-water through Davis Strait. Those for 2004–2006 in the lower part of the table are preliminary. Arctic exports have positive value

Method	Data source	Location	Includes shelves?	Year	Timing	Volume flux (Sv)	Fresh-water flux (mSv)
Geostrophy[a]	CTD section	66.25° N	–	1987	September	5.7	195
Geostrophy[a]	CTD section	66.25° N	–	1988	September	1.5	126
Geostrophy[a]	CTD section	66.25° N	–	1989	September	5.7	286
Currents and geostrophy[a]	Current meters	66.25° N	–	1987–1990	3-Year mean	2.6	92
Currents and geostrophy[a]	Current meters	66.25° N	No	1987–1990	3-Year mean	3.4	130
Currents and geostrophy[b]	Current meters	66.25° N	No	1987–1990	3-Year mean	2.6	99
Currents and geostrophy[c]	Current meters	66.25° N	No	1987–1990	3-Year mean	3.3	120
Currents and geostrophy[d]	Current meters	66.25° N	No	1987–1990	3-Year mean	3.1	
1/12° simulation[e]	Ocean model			1979–2001	21-Year mean		76
Geostrophy[f]	CTD section	Northern line	–	2004	September	2.5	130
Geostrophy[f]	CTD section	Mooring line	–	2004	September	3.1	110
Geostrophy[f]	CTD section	66.25° N	–	2004	September	2.0	98
Geostrophy[f]	CTD section	Southern line	–	2004	September	−0.3	34
Currents[f]	ADCP	Mooring line	–	2004–05	1-Year mean	2.0	–
Geostrophy[f]	CTD section	Northern line	–	2005	September	2.8	–
Geostrophy[f]	CTD section	Mooring line	–	2005	September	2.8	–
Geostrophy[f]	CTD section	66.25° N	–	2005	September	2.5	–
Geostrophy[f]	CTD section	Southern line	–	2005	September	0.9	–
Geostrophy[f]	SeaGlider CTD	Mooring line	No	2006	September	–	72
Geostrophy[f]	SeaGlider CTD	Mooring line	No	2006	September	–	102
Geostrophy[f]	SeaGlider CTD	Mooring line	No	2006	September	–	115

[a]Cuny et al. (2005)

[b]Tang et al. (2004)

[c]Loder et al. (1998)

[d]Ross (1992)

[e]Maslowski et al. (2003)

[f]APL-UW, unpublished data

Seaglider are 93 ± 40 mSv (2,930 km³/year), including shelves and 96 ± 20 mSv (3,030 km³/year), excluding shelves. These values are smaller than those estimated from data in the late 1980s, but the magnitude of error is unknown and likely large.

The fluxes listed are net values. The West Greenland Current has a northward flow of approximately 2 Sv in Davis Strait, and relative to 34.8 reference salinity it carries fresh-water northward at roughly 60 mSv (1,890 km³/year) (Cuny et al. 2005). Therefore, based on Cuny's numbers, the fluxes southward within the Baffin Current are 4.6 Sv and 150 mSv (4,730 km³/year).

Narrow buoyancy-driven flows may carry appreciable fresh-water during summer within 10 km of the Greenland and Baffin coasts. For example, a coastal current fed by ice-sheet run-off along southeast Greenland apparently transports volume and fresh-water at 1 Sv and 60 mSv (1,890 km³/year) during the thaw season (Bacon et al. 2002). Components of the present observational array may detect such currents but will not likely resolve their extent and rate of transport.

The USA–Canada Fresh-water Initiative is addressing the principal challenges to accurate measurement of volume and fresh-water fluxes through Davis Strait. Among these are: (1) a small baroclinic deformation scale that permits decorrelation of flow variations on a scale of order 10 km; (2) a pronounced concentration of fresh-water flux in a thin (25 m) fast-moving surface layer where current and salinity are difficult to measure; (3) the risk to moorings from moving ice keels and icebergs at depths as great as 200 m; and (4) the fresh-water flux carried by pack ice. The initiative has brought new technology to bear on these challenges.

Instruments on six sub-surface moorings measure ice draft (upward looking sonar), ice velocity and profiles of upper ocean current (ADCP) from a relatively safe depth of 105 m, current at specific depths in the lower part of the water column (conventional current meters) and seawater temperature and conductivity from sensors at discrete depths (Fig. 9.28). There are also three bottom-mounted ADCPs paired with temperature-conductivity sensors to measure the full velocity profile in shelf waters, two on the Greenland side and one on the Baffin. There are temperature-conductivity sensors at five additional shallow sites. At some shelf sites (1 in 2004/2005, 2 in 2005/2006, 4 in 2006/2007) there is an additional temperature-conductivity sensor at roughly 25-m depth in a package (IceCAT) developed at APL-UW; because this sensor measures within the low salinity layer near the ice, at significant risk of damage, it relays its data to a recording module at the seabed. If the sensor is snagged by ice, a weak link in the mooring line fails, permitting loss of the sensor while protecting the data module for later recovery.

Seagliders complement the moored instruments by providing fields of temperature and salinity at appropriate spatial resolution, right up to the surface, year-round and without ongoing ship support. The highly resolved hydrography in combination with time series of velocity, salinity and temperature provides a detailed picture of spatial and temporal variation. This information is essential for the accurate estimation of fluxes and of their empirical uncertainty. The measurements are already practical in the absence of pack ice and effort is now focussed on developing acoustic navigation and communication to provide the same capability when ice prevents communication via satellite.
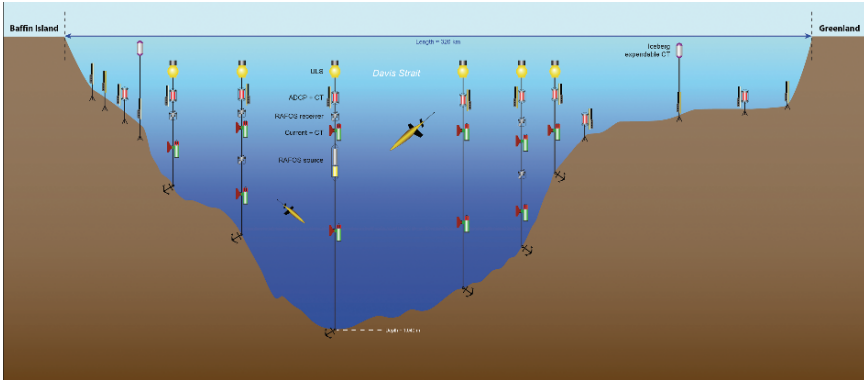
Fig. 9.28 Schematic representation of the array of instruments placed in September 2004 to measure fresh-water flux through Davis Strait
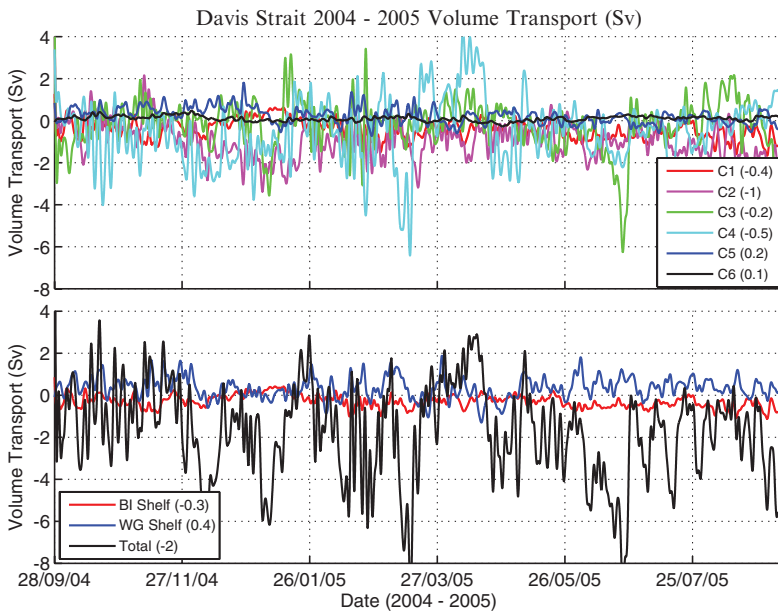
Fig. 9.29 Time series of area-weighted contributions to volume flux through Davis Strait, based on data from individual moorings during September 2004–2005

Although this is a respectable array with instruments at 14 sites and with current measured at 9, the average site spacing of 40 km is still greater than the decorrelation scale of ocean variability (Tang et al. 2004). This is apparent when considering how data from individual moorings contribute to the 2-Sv volume flux for 2004–2005 (Fig. 9.29). The plotted time series are the area-weighted contributions to the

volume flux, each based on data from a single mooring. The time series are obviously poorly correlated with the result that there are long-lived and spurious fluctuations in the estimated flux. The accurate point measurements clearly require the complementary data from Seagliders to resolve variability within the Strait and thereby provide the hydrographic detail needed for intelligent interpolation between time series at fixed and widely spaced locations.

9.11   Summary and Outlook

The tabulation (Table 9.7) of volume and fresh-water fluxes through the gateways for Pacific Arctic through-flow is the outcome of our work in its most concise form.

All of the ASOF initiatives in the North American Arctic are clearly works in progress. Our research is advancing along learning curves in measurement, in interpretation of observations and in modeling. Our confidence to integrate with other ASOF sub-programmes and to explore the impact of global change is growing. Nonetheless, manifest environmental, logistical and technical complexity makes Pacific Arctic through-flow a big topic for research.

The following sections summarize progress towards desired outcomes.

9.11.1   Quantitative Knowledge of Flux Magnitude and Variability

We continue to benefit from promising new observational tools – ADCP, ice-profiling sonar, ICYCLER, IceCat, Sea Glider, methods for direction reference – and developing

Table 9.7 Summary of fluxes through the gateways for Pacific Arctic through-flow, estimated as described in this chapter and subject to many cautions – buyer beware. The value is positive for Arctic out-flow

	Seawater Volume (Sv)	Oceanic fresh-water (mSv)	Ice area (1,000s km²)	Fresh-water as ice[a] (mSv)
Bering Strait	−0.8	−80	–	–
Amundsen Gulf	–	–	−53	−1.7 [1 m]
M'Clure Strait	–	–	−13	−0.8 [2 m]
Sverdrup Basin	–	–	20	2.5 [4 m]
Lancaster Sound	0.7	48	48	1.5 [1 m]
Cardigan Strait and Hell Gate	0.3	–	10	0.3 [1 m]
Nares Strait	0.8[b]	25	33	4.2 [4 m]
Baffin Bay	–	–	690	22 [1 m]
Davis Strait[c]	2.0	100	610	19 [1 m]

[a] Ice thickness has been estimated

[b] Snap-shot in time

[c] Not including flux over the Greenland shelf

numerical models. We have derived new values for fluxes, but values are less forth-coming for fresh-water than for volume. The bias and uncertainty of flux estimates are poorly known. Time series are far shorter than a decade in most instances and are non-existent for fresh-water at some key gateways. In consequence, the tempo-ral overlap of time series within the North American Arctic is not yet sufficient to balance the budgets of Arctic seawater or fresh-water.

9.11.2   *Forcing and Controls on Pacific Arctic Through-Flow*

Researchers favour the steric anomaly of the North Pacific as the prime mover of Pacific Arctic through-flow (Steele and Ermold 2007), but renewed effort to define the magnitude and temporal variation of the absolute geopotential anomaly would be beneficial. Wind may augment or oppose steric forcing. There has been significant recent advance in the understanding of wind amplification in sea straits via mesoscale atmospheric effects and of its consequences for Pacific Arctic through-flow.

Models and observations agree that baroclinicity is an important attribute of Pacific Arctic through-flow. In baroclinic flows the width of low-density boundary currents is comparable to the internal Rossby scale (here about 10 km: Leblond 1980). With this constraint, wider channels cannot necessarily carry larger fluxes. We note that the flux through Lancaster Sound, nearly 70 km wide, is apparently only three times that through Cardigan Strait which has one ninth the width.

Numerical simulation has demonstrated that flow through Nares Strait is strongly influenced by atmospheric forcing that has been amplified via local orography and mesoscale atmospheric dynamics. Measurements of wind and temperature are needed in the planetary boundary layer to evaluate the simulations and to promote the understanding of oceanic and pack-ice responses. Because these processes may be important to through-flow in other areas, there is need for modelling at high reso-lution over a widened geographic domain.

Oceanic flows through the Pacific–Arctic gateways are thought to be controlled by friction and perhaps by rotational hydraulic effects. Numerical simulation of circulation within the Canadian Archipelago using a simple parameterization of drag has illustrated the importance of tidal current as a source of turbulence kinetic energy and therefore of resistance to flow at sub-tidal frequency. Since details are poorly developed, a future focus on these mechanisms in the context of Pacific Arctic through-flow is recommended.

Sea ice, as pack ice or as fast ice, covers the North American Arctic for much of the year. The impact of ice on channel flow is highly non-linear. It can range from an enhancement of wind forcing in the presence of rough mobile pack ice to a complete isolation from wind forcing by fast ice. In the latter instance, the immobile ice sheet exerts additional drag on oceanic flow. We recommend an ini-tiative to understand the intermittent flow and blockage of sea ice in straits, with the ultimate objective of a reliable predictive capability.

9.11.3   Theory and Simulation of Through-Flow

There are many relevant theoretical topics to be addressed, ranging from the practical representation of rotational stratified flow in tidal channels to ocean hydrography and the circulation of fresh-water and sea ice on a hemispheric scale. In particular, we need a clearer notion of the hydrologic asymmetry between the Atlantic and Pacific that creates the steric anomaly that may drive the Pacific Arctic through-flow. An improved theoretical understanding will contribute to the numerical models that must ultimately provide our capability to hind-cast and predict Pacific Arctic through-flow, and to generate spatially complete and temporally continuous perspectives that are inaccessible via direct measurement.

9.11.4   Response to Global Change

The Pacific Arctic through-flow apparently responds to atmospheric and hydrologic forcing on a hemispheric scale. Our understanding of this forcing, of the varying storage of fresh-water within the Arctic Ocean and its ice cover and of the controls on out-flows to the Labrador Sea is not sufficient at present to support plausible hypotheses regarding the impact of changing climate on Pacific Arctic through-flow over the next century.

The practical task of ocean-flux measurement could benefit from continued focus on several issues.

There is need for a proven and agreed methodology for ocean-flux estimation. Table 9.8 summarizes the arrays presently installed in various gateways to measure Pacific Arctic through-flow. With two exceptions, the arrays fail to resolve the flow at the baroclinic Rossby scale (10 km) and all fail to measure salinity in the upper 30 m, where a large fraction of the fresh-water flux occurs (Melling 2000). Two arrays do use a prototype instrument to sample the upper layer, but at too few locations. Table 9.8 joins discussion earlier in the chapter to illustrate that we have yet to justify our methodology for flux measurement. Arrays with

Table 9.8 Summary of the arrays now installed to measure fresh-water flux

	Width of gateway (km)	Number of moorings (current)	Mooring separation (km)	Maximum depth (m)	Number of levels of salinity[a]	Top level of salinity (m)
Bering Strait	76	1–2	38–76	50	1	40
Lancaster Sound	68	2–4	17–34	280	1–3+	30 (5)[b]
Cardigan Strait, Hell Gate	12	2	6	180	1	100
Nares Strait	38	8	5	380	5	30
Davis Strait	360	9	40	1,000	1–3+	50 (25)[b]

[a] '+' indicates more levels measured by prototype near-surface instrument

[b] Shallow depth measured by prototype instrument at one site only

improved resolution of flow structure across sections and improved delineation of shallow salinity structure can assist in this task. The data that we acquire with improved arrays may ultimately provide the justification for the simplifying assumptions that are now being made, a priori.

One expected outcome of a proven methodology is an error model for ocean-flux estimation. Expanded arrays will provide the redundancy required to advance our understanding of sampling error and observational bias. At present we lack the ancillary data to understand why computed fluxes on adjacent sections differ and cannot check the consistency of our results via independent means.

An integrated approach to measuring and modelling the fresh-water fluxes moved as sea ice and as low salinity seawater is strongly advised. Fresh-water cycles between the seawater and ice phases with the annual freeze-thaw cycle as it moves across the North American Arctic. At times the ice and ocean may transport fresh-water in opposite directions. Ice measurements lag those in the ocean except in the aspect of geographic coverage; otherwise, ice velocity is only coarsely resolved in time (3 days) and ice thickness is rarely measured.

The Arctic Sub-Arctic Ocean Fluxes study has recommended a decade of synoptic observation. We have been late starting in the west and the only time series to achieve the 10-year target is that in Bering Strait (Fig. 9.30). The period of synoptic observation at all gateways is 3 years (2003–2006). A prolongation of existing time series is necessary to meet the original ASOF target.

At present we work hard to determine fresh-water flux, perhaps resolved as weekly or monthly averages. However, the ultimate impact of fresh-water in the receiving basins is critically dependent on the form in which it is delivered; the effect of a large seawater flux at salinity near 34.8 is very different from that of a small flux at near zero salinity, such as melting sea ice. In many cases we actually have the data in hand to report histograms of fresh-water flux according to salinity (Melling 2000) – the separate reporting of ice and seawater contribution is a first step. We recommend that a breakdown of the fresh-water flux by salinity become standard practice in reporting.

We are beginning to exploit the potential of trace chemical and isotope anomalies to reveal the sources of fresh-water, decadal variability and the time scales of transit.
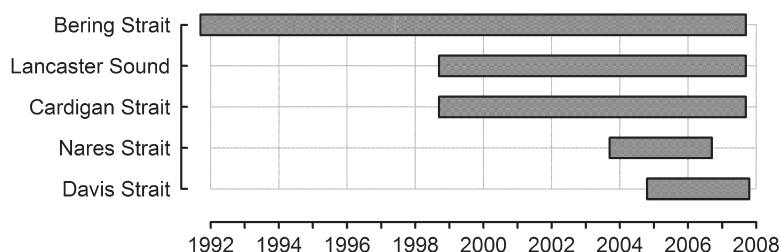
Fig. 9.30 Lifetimes of moored arrays within the gateways for Pacific-Arctic through-flow. The bars span those years during which current was measured for much of the time, but perhaps not in sufficient detail to permit the calculation of fluxes

The reward of this work will increase with the number of repeated geochemical surveys. With caution we can use some of the earlier (1985–1995) data, but sampling and analyses to modern standards have been completed only three times and these during the last decade. At a 3-year repetition interval, change in some components of the ice-ocean system is already aliased. Continued regional surveys, at annual intervals in certain areas, and efforts to resolve the strong seasonal cycles in fresh-water components, are needed to move understanding forward at this time.

There is continuing need for new observational technology. Preliminary work with sea-level signals (via pressure recorders and satellite altimetry) shows promise and should be pursued, in conjunction with programmes of in situ observation. The challenge of measuring fresh-water flux within the top 30 m remains with us – new technological approaches are always welcome. Above all, there is a strong incentive for new instruments and methods that provide needed data at reduced cost.

Ocean circulation models of the Canadian Archipelago are afflicted by shortage in three domains, bathymetry, hydrography and surface meteorology. The first, required to build a realistic geometry for the Canadian polar shelf, is plentiful in some areas, but patchy or non-existent in others. In some areas the need could be addressed by facilitating the migration of existing survey data into an accessible digital archive; in other areas new surveys are required that meet the reasonable needs of numerical simulation – needs that are much more modest than those of navigation. A modest objective for hydrographic information is the acquisition of temperature-salinity data sufficient to prepare a synoptic picture for the entire Canadian polar shelf for each season of the year. From meteorology, we need ocean-relevant observations of surface wind and temperature, to evaluate mesoscale atmospheric models and to promote understanding of the seasonal cycle of sea-ice growth, consolidation, break-up and decay in the largest fast-ice domain in the world.

References

Aagaard K, EC Carmack (1989) The role of sea ice and other fresh-water in the Arctic circulation. Journal of Geophysical Research 94:14485–14498

Agnew TA (1998) Drainage of multi-year sea ice from the Lincoln Sea. CMOS Bulletin 26(4):101–103

Agnew T, AH Le, T Hirose (1997) Estimation of large scale sea ice motion from SSM/I 855 GHz imagery. Annals of Glaciology 25:305–311

Agnew TA, J Vandeweghe (2005) Report on estimating sea-ice transport into the North Atlantic using the Advanced Microwave Scanning Radiometer (AMSR-E). Unpublished report, 21 pp

Agnew TA, J Vandeweghe, A Lambe (2006) Estimating the sea-ice-area flux across the Canadian Arctic Archipelago using the Advanced Microwave Scanning Radiometer (AMSR-E). Unpublished report, 20 pp

Ahlnäs K, GR Garrison (1984) Satellite and oceanographic observations of the warm coastal current in the Chukchi Sea. Arctic 37:244–254

Alkire MB, KK Falkner, I Rigor, M Steele, J Morison (2006) The return of Pacific waters to the upper layers of the central Arctic Ocean. Deep-Sea Research, submitted

Amon RMW, G Budéus, B Meon (2003) Dissolved organic carbon distribution and origin in the Nordic Seas: Exchanges with the Arctic Ocean and the North Atlantic. Journal of Geophysical Research 108, doi:101029/2002JC001594

Bacon S, SG Reverdin, IG Rigor, HM Snaith (2002) A freshwater jet on the east Greenland shelf. Journal of Geophysical Research 107, doi:101029/2001JC000935

Barber FG (1965) Current observations in Fury and Hecla Strait. Journal of the Fisheries Research Board of Canada 22:225–229

Bradley RS, FT Keimig, HF Diaz (1992) Climatology of surface-based inversions in the North American Arctic. Journal of Geophysical Research 97:15699–15712

Bromwich DH, JJ Cassano, T Klein, G Heinemann, KM Hines, K Steffen, JE Box (2001) Mesoscale modeling of katabatic winds over Greenland with the Polar MM5. Monthly Weather Review 129:2290–2309

Cassano JJ, JE Box, DH Bromwich, L Li, K Steffen (2001) Evaluation of Polar MM5 simulations of Greenland's atmospheric circulation. Journal of Geophysical Research 106:33867–33890

Cherniawsky JY, WR Crawford, OP Nikitin, EC Carmack (2005) Bering Strait transports from satellite altimetry. Journal of Marine Research 63:887–900

Clement JL, W Maslowski, LW Cooper, JM Grebmeier, W Walczowski (2005) Ocean circulation and exchanges through the northern Bering Sea: 1979–2001 model results. Deep-Sea Research II 52:3509–3540, doi:101016/jdsr2200509010

Coachman LK, K Aagaard (1966) On the water exchange through Bering Strait. Limnology and Oceanography 11:44–59

Coachman LK, K Aagaard (1981) Re-evaluation of water transports in the vicinity of Bering Strait. In: The Eastern Bering Sea Shelf: Oceanography and Resources vol 1. DW Hood and JA Calder (eds). National Oceanic and Atmospheric Administration, Washington, DC:95–110

Coachman LK, K Aagaard, RB Tripp (1975) Bering Strait: The Regional Physical Oceanography. University of Washington Press, Seattle, WA

Codispoti LA, D Lowman (1973) A reactive silicate budget for the Arctic Ocean. Limnology and Oceanography 18:448–456

Cooper LW, LA Codispoti, V Kelly, GG Sheffield, JM Grebmeier (2006) The potential for using Little Diomede Island as a platform for observing environmental conditions in Bering Strait, Arctic 59:129–141

Cooper LW, TE Whitledge, JM Grebmeier, T Weingartner (1997) The nutrient salinity and stable oxygen isotope composition of Bering and Chukchi Seas waters in and near Bering Strait. Journal of Geophysical Research 102:12563–12573

Cuny J, PB Rhines, R Kwok (2005) Davis Strait volume freshwater and heat fluxes. Deep-Sea Research I 52:519–542

de Lange Boom BR, H Melling, RA Lake (1987) Late Winter Hydrography of the Northwest Passage: 1982 1983 and 1984. Canadian Technical Report of Hydrography and Ocean Sciences No 79, 165 pp. Unpublished report available from Institute of Ocean Sciences Box 6000 Sidney Canada V8L 4B2

Deutsch C, N Gruber, RM Key, JL Sarmiento, A Ganachaud (2001) De-nitrification and N_2 fixation in the Pacific Ocean. Global Biogeochemical Cycles 15:483–506, doi:101029/2000GB001291

Dunphy M, F Dupont, CG Hannah, D Greenberg (2005) Validation of Modeling System for Tides in the Canadian Arctic Archipelago. Canadian Technical Report of Hydrography and Ocean Sciences 243: vi + 70 pp. Unpublished report available from Bedford Institute of Oceanography Box 1006 Dartmouth Canada B2Y 4A2

Ekwurzel B, P Schlosser, RA Mortlock, RG Fairbanks (2001) River runoff sea ice meltwater and Pacific water distribution and mean residence times in the Arctic Ocean. Journal of Geophysical Research 106:9075–9092

Falkner KK, MC O'Brien, H Melling, E C Carmack, F A McLaughlin, A Münchow, E P Jones (2006) Interannual variability of dissolved nutrients in the Canadian Archipelago and Baffin Bay with implications for fresh-water flux. Journal of Geophysical Research Bio-Geosciences, submitted

Fissel DB, JR Birch, H Melling, RA Lake (1988) Non-tidal Flows in the Northwest Passage. Canadian Technical Report of Hydrography and Ocean Sciences No 98:143 pp. Unpublished report available from Institute of Ocean Sciences Box 6000 Sidney Canada V8L 4B2

Gruber N, JL Sarmiento (1997) Global patterns of marine nitrogen fixation and de-nitrification. Global Biogeochemical Cycles 11:235–266

Guo Z, DH Bromwich, JJ Cassano (2003) Evaluation of Polar MM5 simulations of Antarctic atmospheric circulation. Monthly Weather Review 131:384–411

Häkkinen S, A Proshutinsky (2004) Fresh-water content variability in the Arctic Ocean. Journal of Geophysical Research 109 doi:101029/2003JC001940

Holloway G, T Sou (2002) Has Arctic sea ice rapidly thinned? Journal of Climate 15:1691–1701

Jones EP, LG Anderson (1990) On the origin of the properties of the Arctic Ocean halocline north of Ellesmere island: results from the Canadian Ice Island. Continental Shelf Research 10:485–498

Jones EP, LG Anderson, JH Swift (1998) Distribution of Atlantic and Pacific waters in the upper Arctic Ocean: Implications for circulation. Geophysical Research Letters 25:765–768

Jones EP, AR Coote (1980) Nutrient distributions in the Canadian Archipelago: Indicators of summer water mass and flow characteristics. Canadian Journal of Fisheries and Aquatic Science 37:589–599

Jones EP, JH Swift, LG Anderson, M Lipizer, G Civitarese, KK Falkner, G Kattner, FA McLaughlin (2003) Tracing Pacific water in the North Atlantic Ocean. Journal of Geophysical Research 108, doi:101029/2001JC001141

Kahl JD, MC Serreze, RC Schnell (1992) Tropospheric low-level temperature inversions in the Canadian Arctic. Atmosphere-Ocean 30:511–529

Kinney P, ME Arhelger, DC Burrell (1970) Chemical characteristics of water masses in the Amerasian Basin of the Arctic Ocean. Journal of Geophysical Research 75:4097–4104

Kliem N, DA Greenberg (2003) Diagnostic simulations of the summer circulation in the Canadian Arctic Archipelago. Atmosphere-Ocean 41:273–289

Kwok R (2005) Variability of Nares Strait ice flux. Geophysical Research Letters 32 L24502, doi:101029/2005GL024768

Kwok R (2006) Exchange of sea ice between the Arctic Ocean and the Canadian Arctic Archipelago. Geophysical Research Letters 33 L16501, doi:101029/2006GL027094

Kwok R, GF Cunningham, S Yueh (1999) Area balance of Arctic Ocean Perennial Ice Zone: October 1996 – April 1997. Journal of Geophysical Research 104 25747, doi:101029/1999JC900234

Kwok R, A Schweiger, D A Rothrock, S Pang, C Kottmeier (1998) Sea ice motion from satellite passive microwave imagery assessed with ERS SAR and buoy motions. Journal of Geophysical Research 103:8191–8214

Lammers RB, AI Shiklomanov, CJ Vorosmarty, BM Fekete, BJ Peterson (2001) Assessment of contemporary Arctic river runoff based on observational discharge records. Journal of Geophysical Research 106:3321–3334

LeBlond PH (1980) On the surface circulation in some channels of the Canadian Arctic Archipelago. Arctic 33:189–197

Loder JW, B Petrie, G Gawarkiewicz (1998) The coastal ocean off north-eastern North America: A large-scale view. In: The Sea 11:105–133, Chapter 5.

Maslowski W, JL Clement, W Walczowski (2003) Modeled Arctic sub-Arctic ocean fluxes during 1979–2001. Abstract #9554 EGS-AGU-EUG Joint Assembly. Nice, France: 6–11 April 2003

McLaren AS, P Wadhams, R Weintraub (1984) The sea ice topography of M'Clure Strait in winter and summer of 1960 from submarine profiles. Arctic 37:110–120

Melling H (2000) Exchanges of fresh-water through the shallow straits of the North American Arctic. In: The Fresh-water Budget of the Arctic Ocean. Proceedings of a NATO Advanced Research Workshop. Tallinn Estonia. 27 April–1 May 1998. EL Lewis et al. (eds). Kluwer, Dordrecht, The Netherlands, pp. 479–502

Melling H (2002) Sea ice of the northern Canadian Archipelago. Journal of Geophysical Research 107:3181, doi:101029/2001JC001102

Melling H, Y Gratton, RG Ingram (2001) Ocean circulation within the North Water polynya of Baffin Bay. Atmosphere-Ocean 39:301–325

Melling H, PH Johnston, DA Riedel (1995) Measurement of the topography of sea ice by moored sub-sea sonar. Journal of Atmospheric and Oceanic Technology 12:589–602

Melling H, RA Lake, DR Topham, DB Fissel (1984) Oceanic thermal structure in the western Canadian Arctic. Continental Shelf Research 3:233–258

Melling H, DA Riedel (1996) Development of seasonal pack ice in the Beaufort Sea during the winter of 1991–92: A view from below. Journal of Geophysical Research 101:11975–11992

Mosby H (1962) Water salt and heat balance of the North Polar Sea and of the Norwegian Sea. Geophysica Norvegica 24:289–313

Münchow A, H Melling, KK Falkner (2006) An observational estimate of volume and freshwater flux leaving the Arctic Ocean through Nares Strait. Journal of Physical Oceanography 36:2025–2041

Östlund HG, G Hut (1984) Arctic Ocean water mass balance from isotope data. Journal of Geophysical Research 89:6373–6381

Padman L, S Erofeeva (2004) A barotropic inverse tidal model for the Arctic Ocean. Geophysical Research Letters 31 L02303, doi:101029/2003GL019003

Paquette RG, RH Bourke (1974) Observations on the coastal current of Arctic Alaska. Journal of Marine Research 32:195–207

Prinsenberg SJ (1988) Damping and phase advance of the tide in western Hudson Bay by the annual ice-cover. Journal of Physical Oceanography 18:1744–1751

Prinsenberg SJ, EB Bennett (1987) Mixing and transports in Barrow Strait the central part of the Northwest Passage. Continental Shelf Research 7:913–935

Prinsenberg SJ, EB Bennett (1989) Vertical variations of tidal currents in shallow land fast ice-covered regions. Journal of Physical Oceanography 19:1268–1278

Prinsenberg SJ, J Hamilton (2005) Monitoring the volume freshwater and heat fluxes passing through Lancaster Sound in the Canadian Arctic Archipelago. Atmosphere-Ocean 43:1–22

Pritchard RS, RW Reimer, MD Coon (1979) Ice flow through straits. In: Proceedings of POAC'79 vol 3:61–74. Norwegian Institute of Technology, Trondheim, Norway

Proshutinsky AY, M A Johnson (1997) Two circulation regimes of the wind-driven Arctic Ocean. Journal of Geophysical Research 102:12493–412514

Roach AT, K Aagaard, CH Pease, SA Salo, T Weingartner, V Pavlov, M Kulakov (1995) Direct measurements of transport and water properties through the Bering Strait. Journal of Geophysical Research 100:18443–18457

Roff JC, L Legendre (1986) Physico-chemical and biological oceanography of Hudson Bay. In: Canadian Inland Seas. IP Martini (ed). Elsevier, New York, pp. 265–291

Ross C (1992) Moored current meter measurements across Davis Strait. NAFO Research Document 92/70

Sadler HE (1976) Water heat and salt transports through Nares Strait Ellesmere Island. Journal of the Fisheries Research Board of Canada 33:2286–2295

Sadler HE (1982) Water flow into Foxe Basin through Fury and Hecla Strait. Le Naturaliste Canadian 109:701–707

Samelson RM, SJ Lentz (1994) The horizontal momentum balance in the marine atmospheric boundary layer during CODE-2. Journal of the Atmospheric Sciences 51:3745–3757

Samelson RM, T Agnew, H Melling, A Münchow (2006) Evidence for atmospheric control of sea-ice motion through Nares Strait. Geophysical Research Letters 33 L02506, doi:101029/2005GL025016

Sanderson BG (1987) Statistical properties of iceberg motion at the western entrance of Lancaster Sound. In: Proceedings of Oceans'87 MTS/IEEE, vol 19:17–23

Schlosser P, B Ekwurzel, S Khatiwala, B Newton, W Maslowski, S Pfirman (2000) Tracer studies of the Arctic fresh-water budget. In: The Fresh-water Budget of the Arctic Ocean. EL Lewis (ed). Kluwer, Dordrecht, The Netherlands, pp. 453–478

Serreze MC, AP Barrett, AG Slater, RA Woodgate, K Aagaard, R Lammers, M Steele, R Moritz, M Meredith, CM Lee (2006) The large-scale fresh-water cycle of the Arctic Journal of Geophysical Research, submitted

Smith JN, KM Ellis, T Boyd (1999) Circulation features in the Central Arctic Ocean revealed by nuclear fuel reprocessing tracers from SCICEX 95 and 96. Journal of Geophysical Research 104:29633–29677

Sodhi DS (1977) Ice arching and the drift of pack ice through restricted channels. CRREL Report No 77–18. US Army Cold Regions Research and Engineering Laboratory Hanover NH. Available NTIS, 11 pp

Steele M, W Ermold (2007) Steric sea level change in the northern seas. Journal of Climate 20:403–417

Steele M, D Thomas, D Rothrock, S Martin (1996) A simple model of the Arctic Ocean fresh-water balance 1979–1985. Journal of Geophysical Research 101:20833–20848

Stigebrandt A (1984) The North Pacific: a global-scale estuary. Journal of Physical Oceanography 14:464–470

Strain PM, FC Tan (1993) Seasonal evolution of oxygen isotope-salinity relationships in high-latitude surface waters. Journal of Geophysical Research 98:14589–514598

Tang CL, CK Ross, T Yao, B Petrie, BM DeTracy, E Dunlop (2004) The circulation water masses and sea ice of Baffin Bay. Progress in Oceanography 63:183–228

Taylor JR, KK Falkner, U Schauer, M Meredith (2003) Quantitative considerations of dissolved barium as a tracer in the Arctic Ocean. Journal of Geophysical Research 108, doi:101029/2002JC001635

Tremblay J-É, Y Gratton, EC Carmack, CD Payne, NM Price (2002) Impact of the large-scale Arctic circulation and the North Water polynya on nutrient inventories in Baffin Bay. Journal of Geophysical Research 107, doi:101029/2000JC000595

Weingartner TJ, SL Danielson, TC Royer (2005) Fresh-water variability and predictability in the Alaska Coastal Current. Deep-Sea Research II 52 169–191, doi:1101016/jdsr1012200410091030

Wijffels SE, RW Schmitt, HL Bryden, A Stigebrandt (1992) Transport of freshwater by the oceans. Journal of Physical Oceanography 22:155–162

Williams CE, W Maslowski, JC Clement, AJ Semtner (2004) Fresh-water Fluxes from the Arctic into the North Atlantic Ocean: 1979–2002 model results. American Geophysical Union Fall Meeting 2004 2004AGUFMC54A-05W

Winant CD, CE Dorman, CA Friehe, RC Beardsley (1988) The marine layer off northern California: An example of supercritical channel flow. Journal of Atmospheric Sciences 45:3588–3605

Woodgate RA, K Aagaard (2005) Revising the Bering Strait fresh-water flux into the Arctic Ocean. Geophysical Research Letters 32 L02602, doi:101029/2004GL021747

Woodgate RA, K Aagaard, TJ Weingartner (2005a) Monthly temperature salinity and transport variability of the Bering Strait through-flow. Geophysical Research Letters 32 L04601, doi:101029/2004GL021880

Woodgate RA, K Aagaard, TJ Weingartner (2005b) A year in the physical oceanography of the Chukchi Sea: Moored measurements from autumn 1990–1991. Deep-Sea Research II 52:3116–3149 101016/jdsr2200510016

Woodgate RA, K Aagaard, TJ Weingartner (2006) Inter-annual changes in the Bering Strait fluxes of volume heat and fresh-water between 1991 and 2004. Geophysical Research Letters 33 L15609, doi:101029/2006GL026931

Yamamoto-Kawai M, N Tanaka, S Pivovarov (2005) Fresh-water and brine behaviors in the Arctic Ocean deduced from historical data of $\delta^{18}O$ and alkalinity (1929–2002). Journal of Geophysical Research 110, doi:101029/2004JC002793

Yamamoto-Kawai M, FA McLaughlin, EC Carmack, S Nishino, K Shimada (2006) Fresh-water budget of the Canada Basin Arctic Ocean from geochemical tracer data. Journal of Geophysical Research, submitted